Contactless monitoring of the newborn's Heart Rate

Valeria Pedone

Politecnico di Torino

Supervised by

Filippo Molinari

ISMB tutor

Marco Gavelli

Academic Year 2017/2018

Dedication

To all newborns, our future

Table of contents

Chapter 1

Introduction

The clinical needs underlying the project are mainly two: on one hand, starting from the previously work carried out on the assessment of pain in newborns [12], the objective of this work is to make the measurement of the physiological parameters that contribute to it automatic and objective; on the other hand, it was decided to make non-invasive the measurement of one of the most indicative vital parameters among those continuously monitored in the intensive care unit: the Heart Rate.

1.1 Neonatal Pain

Studies have shown that the newborn, even if preterm, experiences pain and preserves the memory of pain experienced during the neonatal age. [28].

Furthermore, research has demonstrated that acute and repetitive pain in one early stage of development of the nervous system can lead to physiological, cognitive, behavioral, hormonal and endocrine alterations, with consequent harmful effects in the short and long term [24].

The *Ministero della Salute* has set up a commission for the drafting of the Law N.38 of 15 March 2010: *Provisions to guarantee access to treatment palliative and pain therapy.* Article 7 states that: *characteristics of the detected pain and its evolution in the course of hospitalization, within the medical record, in the medical and nursing sections, in use at all health facilities, must be reported as well as the antalgic technique and the drugs used, the relative dosages and the antalgic result achieved* [30].

As a consequence the pain, in the newborn and in the hospitalized subjects, must systematically detected and monitored as the fifth vital parameter by means of validated scales for procedural pain. It must be reported in clinical record of all newborns subjected to procedures deemed to be painful, routine, mandatory or

investigations [24].

Given the inability of the newborn to verbally express the pain, the quantitative assessment of neonatal pain is extremely difficult and relies mainly on the evaluation of crying, the observation of facial grimaces and movements (e.g. limb retraction) and the detection of physiological parameters changes (oxygen saturation and heart rate).

To date, the choice for evaluation is left to health professionals and is therefore very subjective.

There are several pain assessment scales, each refers to different parameters and assigns different scores.

We focused on the PIPP scale, which considers seven parameters: two of which are behavioral (facial expressions), two physiological (heart rate and oxygen saturation) and two contextual ones (gestational age and behavioral state).
Each physiological and behavioral parameter can be assigned a score between 0 and 3, which describes the variation of the parameter analyzed with respect to the rest condition.
The maximum score obtained with PIPP is 21 for premature infants with less than 28 weeks and 18 for newborn infants.
A total score greater than or equal to 6 is associated with painful procedures [24].

1.2 The Heart Rate

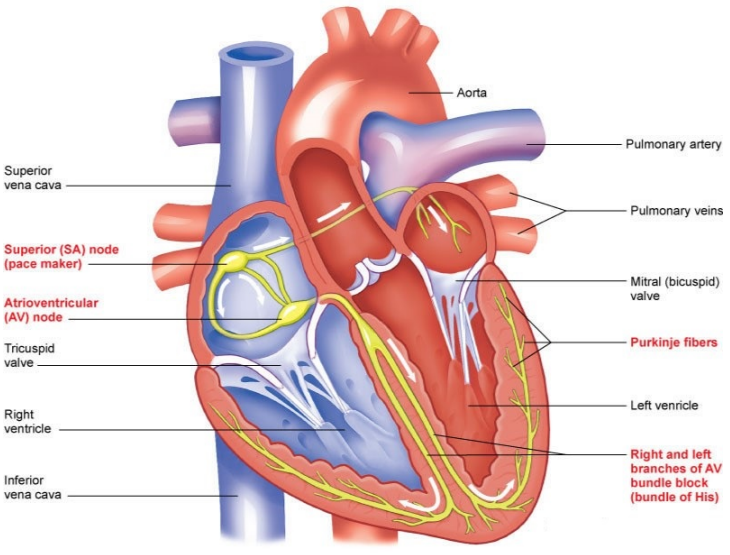

Figure 1.1: the heart, a detail

The heart (fig. 1.1) is a muscular organ with four cavities: left and right atria, which receive blood returning to the heart from the blood vessels, and the right and left ventricles that instead pump blood into the vessels.
The fibers of the heart muscle that make up the conduction system are specialized in generating action potentials and quickly leading them through the myocardium. The contractions of the heart are activated, in a rhythmic and regular way, by action potentials originating in the pacemaker cells distributed in specific regions of the myocardium.
The pacemaker cells of the sino-atrial node in the upper part of the right atrium, in particular, determine the heart rate.

Therefore, the heart rate (HR) represents the heartbeat and it's a measure of the number of heart beats per unit of time, generally beats per minute (bpm).

Depending on the activities carried out, the organs need a variable amount of oxygen: the body responds by adapting to the new physiological conditions by varying the heart rate and inducing vasodilation or vasoconstriction to modulate the amount of blood that irradiates organs and tissues.

The change in heart rate is regulated by the integrated and opposite action of sympathetic and parasympathetic nervous systems, which regulate the involuntary functions and also from the levels of circulating adrenaline hormone (1.2).
The sympathetic system is responsible for the increase in heart rate by induction of the sino-atrial node, while the decrease in heart rate is attributable to the release of acetylcholine on the breast-atrial cells by the vagus nerve stimulated by the parasympathetic system [27].

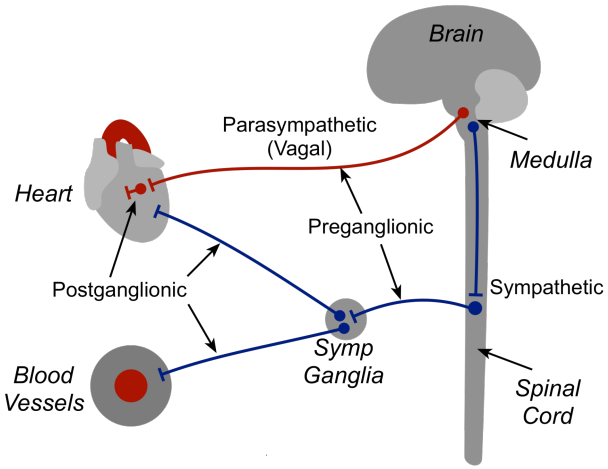

Figure 1.2: cardiac innervation; source: *Cardiovascular Physiology Concepts*

The heart rate varies in different physiological ranges depending on the age, the state of health and, equal to these, depending on many other emotional factors and

related to the lifestyle led.

In general, events in which the heart rate exceeds the upper limit of the physiological range are called tachycardia events; vice versa, when the heart rate falls below the lower physiological limit for the subject, bradycardia occurs.

1.2.1 HR in newborns

In the first days of life of newborns, heart rate and oxygen saturation are indicative parameters to be able to identify and diagnose any diseases and congenital heart defects, for example an out-of-range HR could underlying heart disease or lung problem.

Based on [26], in fact, Heart rate (HR) is the most important clinical indicator to evaluate the status of a newborn, and is also used in any resuscitation efforts as a guide.

In addition, during the first minutes of life in infants needing resuscitation, HR may also be a predictor of early neonatal mortality and moderate to severe brain injury in those who survive [29].

With regard to out-of-range events, a bradycardia situation is generally more alarming for a newborn than a tachycardia.
In both cases, the anomaly may be indicative of various pathologies: a high heart rate may refer to cardiomyopathy, metabolic or other disorders; while a low pulse rate can indicate high intracranial pressure, hypoxia, congenital heart block.
To restore the physiological pulse rate in a highly bradycardic case, however, a sore treatment of chest compression and assisted ventilation is required, which involves intubation and medications.

Each child is subjected, within at least 24 hours after birth, to a screening performed with a pulse oximeter to look for serious congestion.
Following the parameters observed during screening, if deemed necessary, the child can be transferred to the neonatal intensive care unit (NICU) in an incubator, to be able to continuously monitor its vital parameters and observe non-physiological variations.

1.3 Thesis purpose: neonatal HR Monitoring

The aim of the thesis is to estimate in a contactless way the heart rate value of healthy children born at term (gestational age 37-41 weeks), as a starting point to be extended to the NICU.

It is proposed an alternative method to the pulse oximeter used in the neonatology ward, equally based on the extraction and analysis of the photoplethysmographic signal, but without contact with the patients.
By generalizing, ambient light is used as a light source and the sensor of a video camera as a photoreceptor.

The study was carried out by acquiring recordings of children's face during the period of waking or spontaneous sleep - prior parents consent.
The videos have been analyzed to extract signals that represent the variations of light absorbed and reflected by the blood over time, referring to oscillations of the cardiac cycle.
By processing and analyzing the signals in the frequency domain, it was possible to identify the frequency of heartbeats per unit of time.
The estimated values were finally compared with those of the pulse oximeter to evaluate the reliability of the proposed algorithm (see fig.1.3).

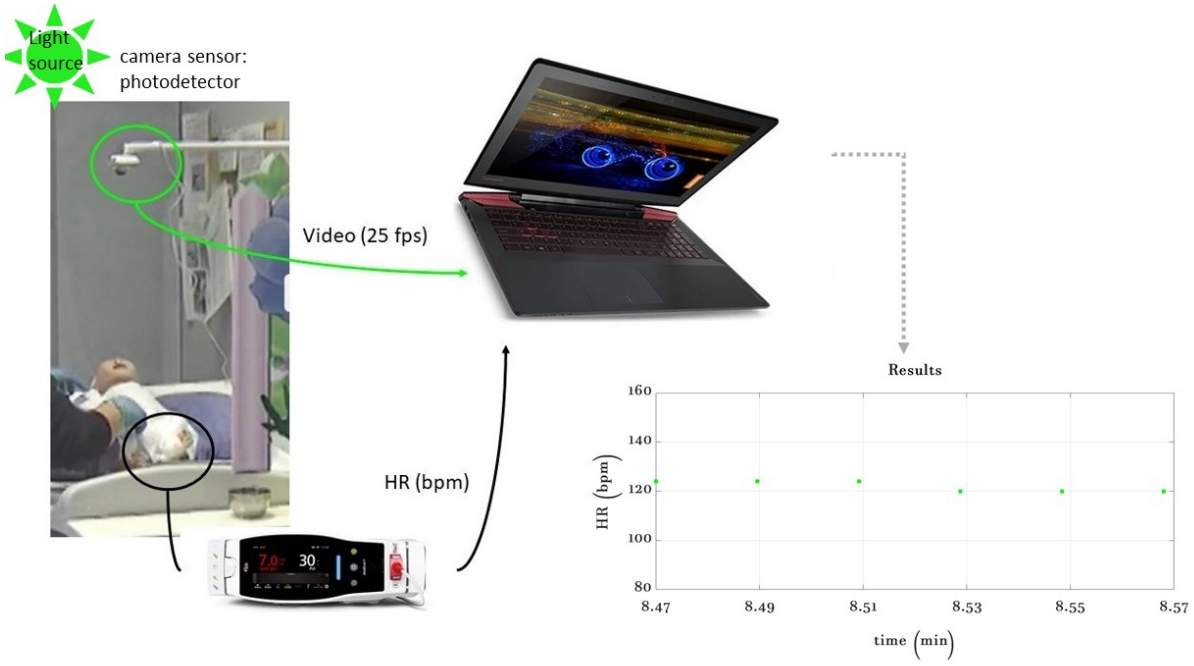

Figure 1.3: overview: reference data and recorded video are the inputs, as output of the processing the comparison between estimated and collected HR values

In the proposed architecture, RGB imaging techniques were adopted, inspired by the methods presented in [13] [14] [15] and in [8], [10], [25] for the specific application to the neonatal clinical environment.

In general, the processing of the signals obtained by averaging pixel intensity of selected skin-exposed area from frames over time, consists of a *detrending* step

(aimed at attenuating the DC component) and of a *filtering* to isolate the frequency band of interest relative to the physiological range.
The heart rate value is then identified as corresponding to the maximum peak of the power spectrum of the processed signal.
The results were estimated with a frequency equal to that of the pulse oximeter sampling, from which the ground truth could be downloaded via software.

This work makes, through encouraging results, a contribution to the research and development of a contactless and reliable method for the evaluation of the heart rate in a non-invasive way in the clinical setting, albeit with limitations.

With regards to neonatal pain, it is necessary to take into account that heart rate is only one of the parameters that contributes to the evaluation, and must be integrated with oxygen saturation, analysis of facial movements and possible crying analysis (as specified in PIPP scale).

It should also be considered that in the application of the contactless method to newborn patients, movement becomes an important aspect: in literature there are in fact many results obtained on adults, often volunteers, who are asked to remain still and frontal with respect to the camera.

In the few experiments done on newborns, it is necessary to identify valid periods in which the subjects are relatively still and frontal.

Some problems, as the selection of the region of interest, were manually solved for the moment, but require future further implementation developments aimed at automation.

1.4 Thesis Structure

The thesis is organized as follows:

- The ”Literature Review” section shows in more detail references to publications and works for the determination of the state of the art and the inspiration for the methods used and reworked for the specific application.

- The ”Clinical Needs” section is dedicated to the clinical needs and problems that motivated the research project.

- The ”Dataset” section illustrates the set up and the used instrumentation, both for video recordings and for processing.

- In the ”Architecture” section the architecture of the work is described, specifying which choices have been made and why.

- In the ”Setup” section the used instrumentation for the recordings is described and the ground-truth providing device is shown.
- In the ”Clinical Study Design” chapter, information about the patient population and the privacy aspect in a clinical environment are given.
- The ”Experimental Results” section presents the results obtained and the methods of analysis used to validate them.
- The ”Future Works” section is dedicated to possible improvements and optimizations of the presented method and future development prospects.
- The ”Conclusion” section summarizes the purpose and the evaluations related to its achievement and a brief discussion on future perspectives.

Chapter 2

Literature Review

2.1 Introduction to Photoplethysmography

Evaluation of the cardiovascular system and vital parameters such as heart rate, respiratory rate and oxygen saturation in the blood are of fundamental importance in the medical field, in terms of monitoring, prevention and diagnosis.

Technological development, adapted to the medical field, has allowed to optimize the time and costs of some procedures, to support the doctors and to face problems that would have been difficult or even impossible to analyze.

Pulse oximetry (p-ox) is an example of a less invasive method than arterial blood gas analysis and ECG, which is quite safe, convenient and inexpensive to be valuable for measuring oxygen saturation (spO2) and heart rate (HR) in some clinical use [5].

Commonly, p-ox is applied in a *transmissive* mode: a light source (id est a LED) is placed on a thin part of the patient's body and transmits through tissue at two wavelengths to a photodetector. It measures the changing absorbance at each of the wavelengths, allowing it to determine the absorbances due to the pulsing arterial blood alone, excluding venous blood, skin, bone, muscle, fat.
Less commonly, *reflectance* pulse oximetry is used: in this case, the light source and the photodetector are closely positioned and just the reflected light is detected to determine pulsing rates (see examples in fig. 2.2).

The purpose of this work is to implement a completely non-invasive remote method to estimate HR value, based on pulse oximetry technology. As experimented in the most recent works, the method of reflection is exploited and the signal of interest investigated is the photoplethysmographic one.

Photoplethysmography is based on the study of the diffusion of different wavelength rays in the tissues, to study their vascular spraying.

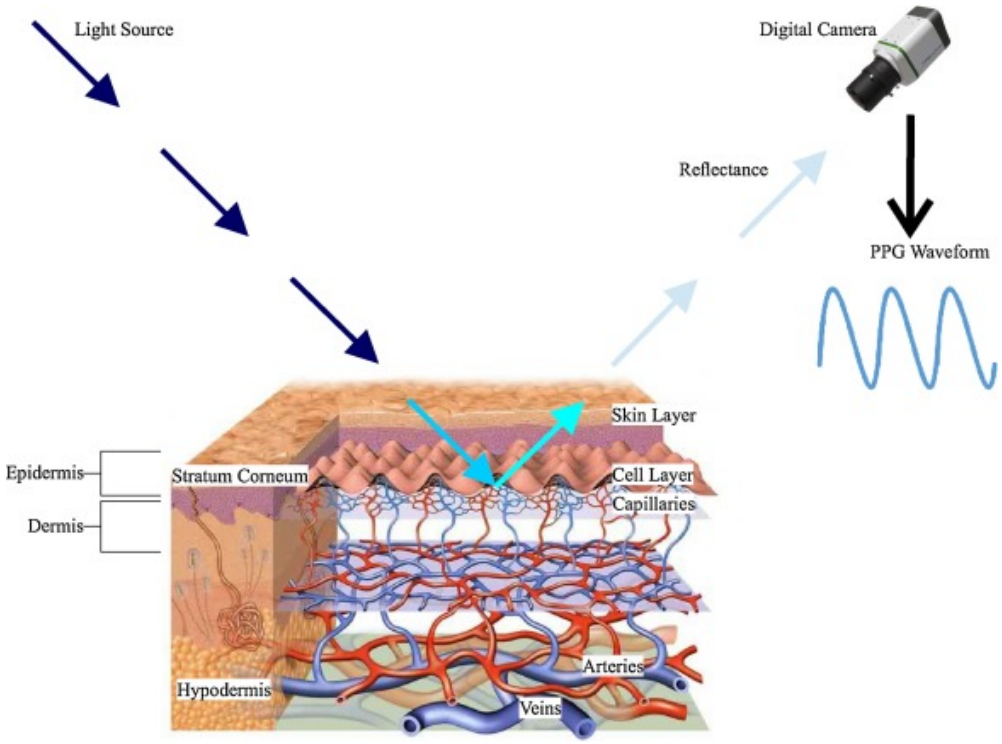

Figure 2.1: Pulse oximetry technology: the optical properties of absorption and reflection of the blood are exploited, different in case of oxygenation and deoxygenation. Skin is exposed at a light source (or two at different wavelengths) and the reflected light is intercepted by the sensor (photodiode in the traditional mode or in this case the camera) to obtain a representative curve of the physiological oscillations due to the cardiac cycle. image source: *Heart rate estimation using facial video: A review*

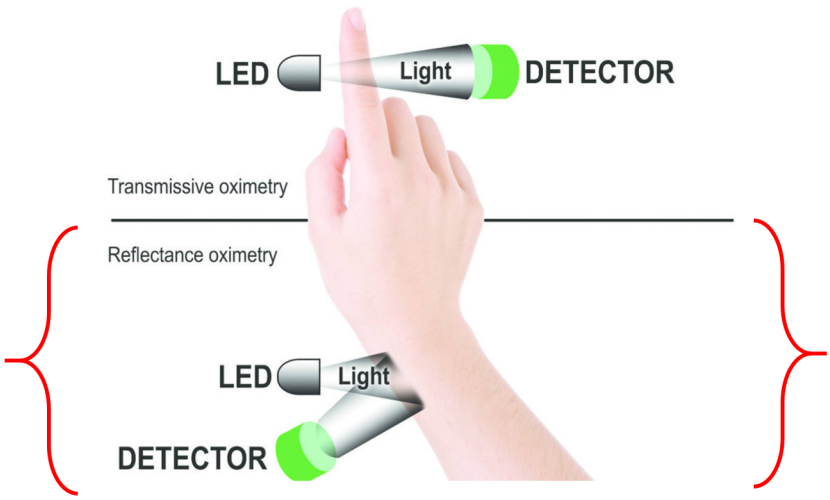

Figure 2.2: example of light source and photoreceptor positioning in transmissive and reflectance oximetry

"The photoplethysmographic (PPG) waveform, also known as the pulse oximeter waveform [...] is an amplified and highly filtered measurement of light absorption by the local tissue over time. It is optimized by medical device manufacturers to accentuate its pulsatile components. Physiologically, it is the result of a complex, and not well understood, interaction between the cardiovascular, respiratory, and autonomic systems" [4].

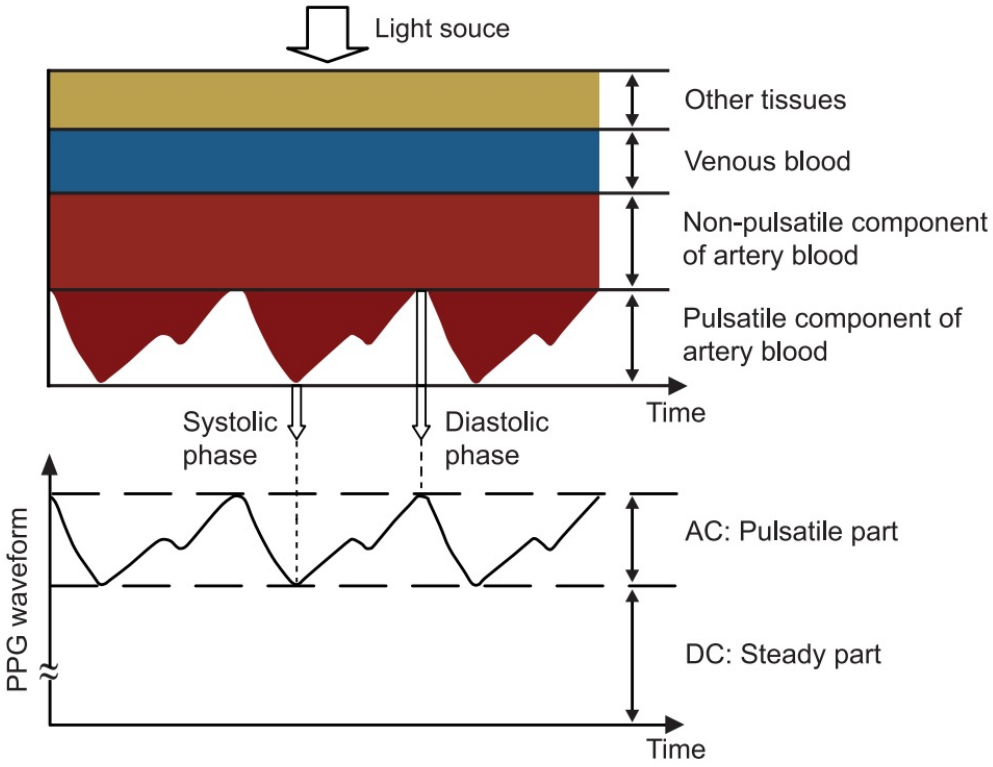

Figure 2.3: example of variation in light attenuation by tissue; PPG waveform [18]

2.2 State of Art

The concept of photoplethysmography (PPG) applied to the human body, based on the methods proposed in the thesis, dates back to about 1930, when Hertzman *et al.* observed the volumetric variations due to the vascularization of human tissues [19].

Over the years, various techniques have been used for the extraction of the photopletysmographic (PPG) signal. A huge amount of information it's contained, compared to the oscillations related to respiration, heartbeat and optical properties of blood, different between oxygenated blood and deoxygenated.

Some examples of experimented techniques are: laser Doppler Imaging [7], laser speckle imaging [2], photoacoustic tomography [11], tissue viability imaging [6].

PPG Imaging is the technique that in the last years has been mostly used for its relative implementation simplicity, for the use of cheap instruments and for the possibility of identifying movement artifacts and application to different areas of the body.

In 2005, Wieringa *et al.* presented a first attempt to extract, from videos acquired at different wavelengths on 7 healthy volunteer adults, PPG signals that contained information on heart rate, respiratory frequency and oxygen saturation.
The proposed algorithm is based upon the detection of a two-dimensional matrix of spatially resolved optical plethysmographic signals. Recordings were processed by dividing each image frame into Regions of Interest (ROIs), then averaging ROI pixels. For each ROI, pulsatile variation over time was assigned to a matrix of ROI-pixel time traces. HR was estimated on the Fourier power spectrum.
Results showed that further development was necessary to apply the method in a clinical environment [17].

In 2007, Humphreys and Ward compared their PPG camera based method to conventional finger pulse oximeter on ten adult volunteers. Even in this case, the region of tissue of volunteers were alternately illuminated with different wavelengths of light, and the backscattered photons were detected by the camera.
PPG signals obtained, after a calibration procedure, resulted comparable with the ones of the reference [20] .

Verkruysse *et al.* showed results on heart rate and respiratory rate estimation by selecting a region of the videotaped face of volunteers, using both ambient light and artificial light as a source of illumination in 2008.
Recordings of the duration from thirthy seconds to several minutes were taken with an inexpensive camera; period of time representing still subjects were selected and region of interest of the forehead were chosen.
A spatial averaging followed by digital filtering and spectral analysis constituted the processing that led to satisfactory results [16].

Between 2010 and 2011, Poh *et al.* presented a method based on webcam acquisitions of the face of twelve participants, whose heart rate, respiratory rate and heart rate variability were extracted with good results.
The novelty of this work concerned the automatic face tracking along with blind source separation of the camera color channels into independent components.
This method is also motion-tolerant and capable of performing concomitant measurements on more than one person at a time [13] [14].

Wu *et al.* presented a video-based method for determining oxygen saturation

using ambient light at two different wavelengths in 2008.
The new method allowed, for the first time, non-contact oxygen saturation measurements by using ambient light with their respective visible wavelength of 660nm and 520nm which is free from interference of the light in other bands [9].

In 2015, Guazzi *et al.* presented a method to measure oxygen saturation using a RGB camera in 5 healthy volunteers; the particularity of this work is that subjects were recorded in a purpose-built chamber over 40 minutes each [3] .

Many of the works cited, which have very encouraging results, are experiments done on volunteers, adults and healthy people.

For the particular application in the clinical field, the most inspiring publication is the one of Tarassenko *et al.*, that in 2014 estimated the respiratory, cardiac, and oxygen saturation frequency of 46 patients during 133 dialysis sessions using a non-contact, video-based method and using ambient light [15].

As regards neonatal pain, the more general area in which this thesis is inserted, the state of the art is represented by [12] :through facial segmentation of newborns and automatic detection of facial landmarks, parameters of specific expressions of the baby were evaluated for painful events. Subsequently, this information are integrated with others, based on the different scale, and a score of pain assessment is determined. For the specific case of PIPP scale, facial information are integrated with those deriving from the monitoring of physiological parameters such as the change in heart rate and in oxygen saturation and a score between 0 and 21 is given.

Some neonatal vital signs monitoring experiments have been presented in recent years:

in 2012, Scalise *et al.* measured the heart rate of 7 infants in intensive care (NICU) starting from acquisitions made with a webcam. Newborns were illuminated by a large light source band and the webcam was positioned 1 meter away from the patients' faces. Each subject was monitored 8 times for about 30 seconds and the reference data were derived from ECG. The heart rate was estimated using an ICA (Independent Component Analysis) based algorithm.
The JADE (joint approximate diagonalization eigenmatrices) method was also implemented to reject motion artifacts.
This is a first example of a work that aims to the reduction of the direct contact with the patient skin in NICU: obtained results show a correlation between the two data sets with a data dispersion that in the ninety-six % of cases is within the limits of agreement of the Bland-Altman plot.

In 2013, a pilot study on non-contact heart rate monitoring in NICU based on camera photoplethysmography was conducted on 19 infants in two NICUs respectively of California and the Netherlands.

Two different patients skin Region of Interest (ROI) were chosen for every patient to detect and track motion artefacts. Average pixel value was calculated and variations in amplitude were interpreted as the result of the cardiovascular pulse wave through the cutaneous blood vessels. Plethysmograms were visualised as joint-time-frequency diagrams (JTFDs). HR related to PPG signal was identified for all the newborns albeit not continuously; infant motion and poor illumination conditions disturbed in fact the acquired signals.
The results of this study are quite good, looking at the Bland-Altman analysis computed [10].

In 2014, a method to monitor continuously pulse rate of patients in neonatal intensive care unit was proposed.
Some of the new features compared to other jobs is the use of a high definition webcam and the extraction of the PPG signal from several regions of interest simultaneously to compensate for any movement artifacts.
Eight infants were monitored at a distance of at least one meter from the webcam for approximately 30 minutes uninterrupted. The algorithm includes, in contrast to other methods, signal interpolation, smoothing and stitching steps to improve the performance of the spectral estimation. Motion compensation was made based on the choice of a signal amplitude threshold.
The estimated heart rate results obtained, show a comparability with those of reference, assessed by means of Bland-Altman analysis [25].

In 2017, another study was made to monitor heart rate, respiratory rate and potentially oxygen saturation of seven babies in the NICU.
To estimate the HR value, a sensitive color video camera and an RGB color magnification were applied while for the estimation of the RR a thermal camera was used exploiting the IR-termography. A tracking software was developed to identify baby movements.
The results were shown on selected periods in such a way that the patients were still and there were no high variations in the reference data (HR and RR considered constant).
The conclusions show that the methods are effective but only under specific conditions: a lot of work still needs to be done to achieve a real-time system for long-term monitoring [23].

In 2017, Jorge et al monitored the respiratory rate of 30 pre-term children born for 4 consecutive days in NICU, also developing a classification system for respiratory cessation events (COBE) [21].
What is interesting is the used setup, which provided for the insertion of the camera directly into the incubator, prepared with a special hole.

The extraction of the PPG signal is similar to the other works presented for the estimate of the heart rate: oscillations related to the respiratory act and to a different absorption of light by the blood depending on the saturation are in fact contained. Subsequently, the blue channel is analyzed mainly, unlike what is done for HR (green channel).

Chapter 3

Architecture

3.1 Introduction

The purpose of the present work is a non-contact approach for estimating heart rate of healthy infants, as an alternative to the contact pulse oximeter used in practice in some hospital wards; the project is inserted into the more general context of the objective assessment of neonatal pain.

The method is based on photoplethysmographic optical technology, as reported in chapter "**Literature**".

Ambient light is the 'light source' and the sensor of the video camera is the 'photoreceptor' (see fig. 3.1).

3.2 Overview of the estimation process

The proposed architecture is shown in 3.1

At the beginning, on the first frame, the face is selected defining a box around it manually.

The intensity of the pixels for the three colour channels from the box are then averaged to obtain signals that represent changes over time.

The variations in amplitude from the extracted signal are verified to be attributable to physiological oscillations, both visually and automatically.

Starting from these tests, a quality index of the time interval is defined, on the basis of which invalid periods are excluded.

For each valid period, a region of interest (ROI) is manually defined on the first frame analogously to the first step for the face.

Intensity of the ROI pixels for the green channel are averaged to obtain again signals that represent changes over time (particularly the cardiac pulse).

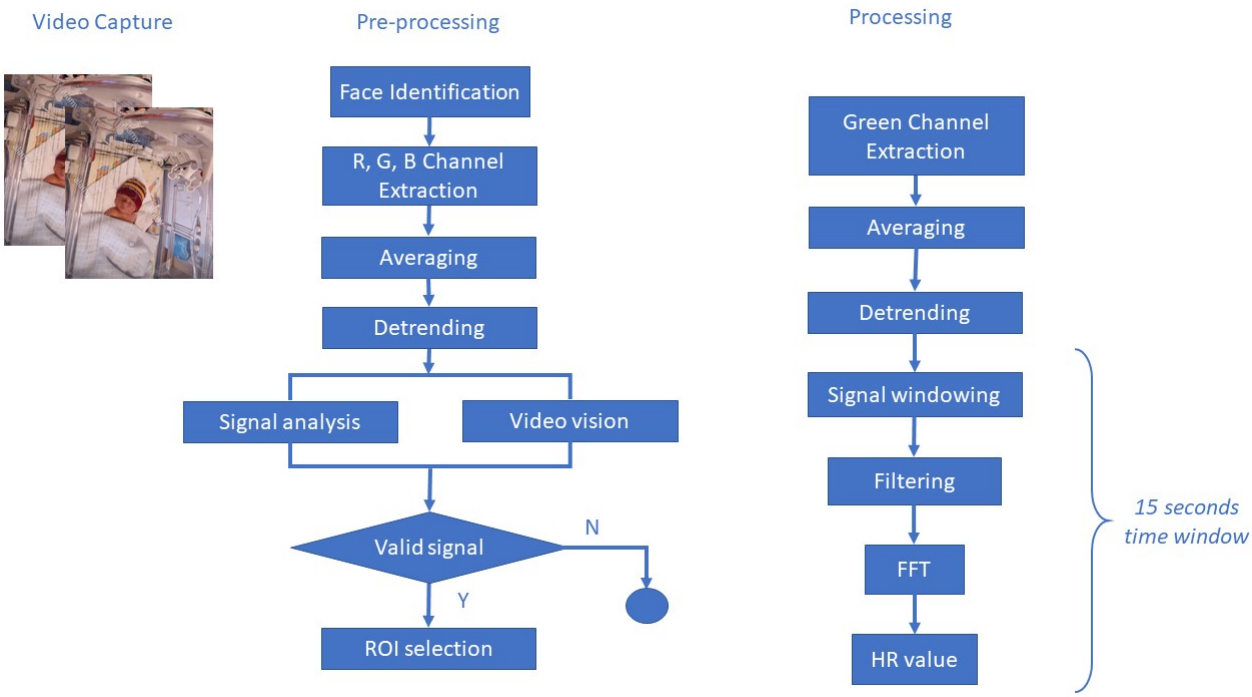

Figure 3.1: block diagram of processing steps towards the estimation of heart rate from neonatal video data. ROI = region of interest; R,G,B = Red, Green, Blue; FFT = Fast Fourier Transform

Finally, to estimate heart rate values, the signal in the frequency domain is analyzed. The spectrum has to contain relevant information in the physiological range, therfore low frequencies due to the direct component of the signal are attenuated by *detrending* and 'out-of range' frequencies are attenuated by *filtering*.
The heart rate - in beats per minute (bpm)- is computed as the frequency corresponding to the highest peak of the Fast Fourier Transform (FFT), multiplied by 60.

Details for each block are given below.

3.3 Implementation

3.3.1 Face identification

The face of the infant is manually selected as a box and parametrised:

- *abscissa* and *ordinata* of upper-left corner of the box
- *width*
- *height*

Figure 3.2: Example of face selection, subject 7

3.3.2 Averaging

Computing the mean of all the pixels in the selected box, for each colour separately, allows to observe oscillations of pixel intensities over time. It was expected the three color channels to contain different information; the green channel signal to represent cardiac pulse better than the blue and the red ones: as detailed in [16], the three obtained signals contain information related to different signals: the green channel represents the variations of light absorption and reflectance during the cardiac cycle, while information on the respiratory rate are more easily identifiable in the red and the blue channels.

In figure 3.3 it is possible to observe in time domain that the green channel it is more representative of cardiac pulse respect to red and blue ones. From this point on, only the signal related to the green channel will be processed.

3.3.3 Detrending

Once the signal has been averaged, it has been detrended to attenuate the continuous component (DC) and to ”flatten” any slowly increasing or decreasing oscillations.

As a general rule, it may be convenient to subtract the mean value or a best linear fit to the data; in this specific case, slow variations appear to have a linear trend.

The *detrend* function of MATLAB proved to be effective for this specific purpose in order to remove linear trends.

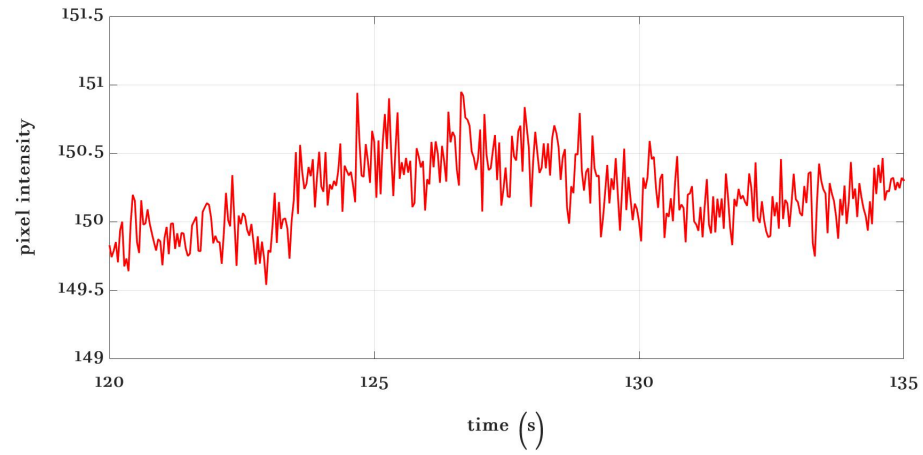

(a)

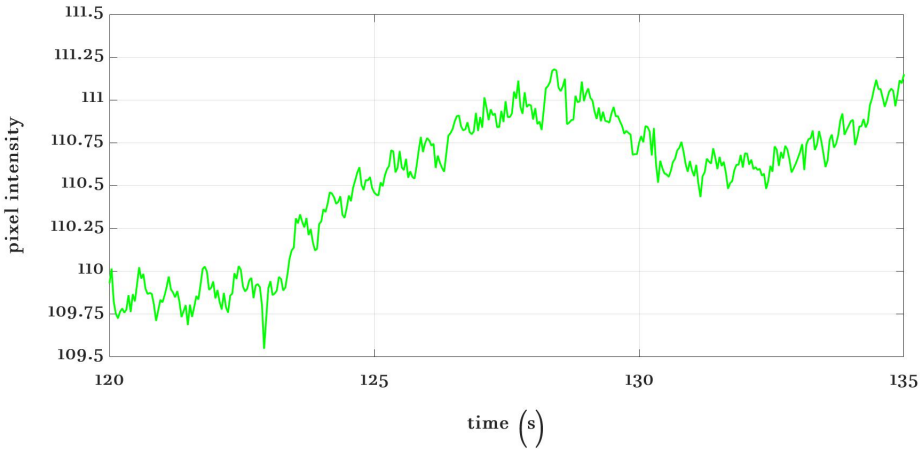

(b)

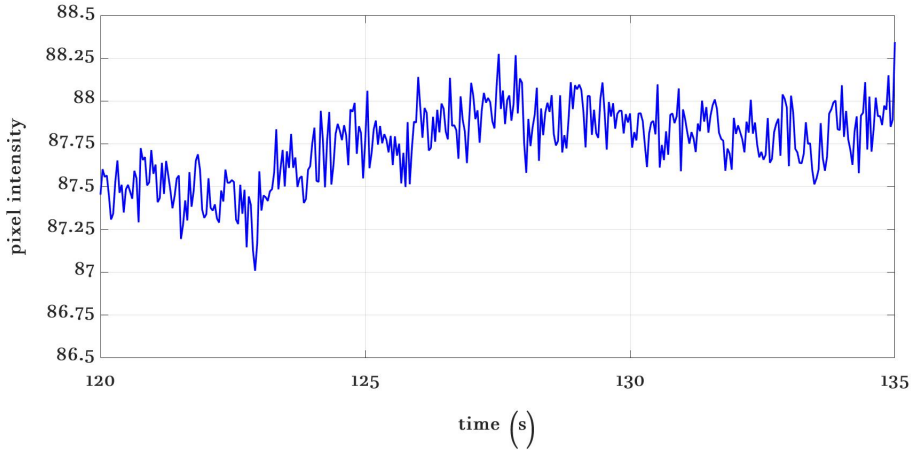

(c)

Figure 3.3: Output of the signal, averaging step (15-second detail, subject 8): (a) raw trace obtained averaging pixels value in channel: RED, (b) GREEN, (c) BLUE

3.3.4 Signal validation

From the signals obtained as output of the averaging step (see fig. 3.3), I also expect to observe high amplitude variations, over entire signal, potentially representative of movements of the infant face or changing in ambient light.

As mentioned in section "Overview" , the verification of the validity of the periods is performed either manually, watching the videos, and automatically: the traces obtained have consecutive peaks of heigth equal to 5-7 pixels when representative of the cardiac pulse, while in close proximity to child movements or changing in ambient light, the width of the peaks is higher than 7 pixels.

A quality index is then assigned to the time intervals (see fig. 3.4).

Note that, to qualify a period as 'invalid', it's enough to intercept a first peak of amplitude higher than 7 pixels; instead to qualify a period as 'valid', sequences of successive peaks of amplitude included in the 7 pixels must follow one another for a number of samples equal to at least 15 seconds, the chosen time window for estimating the HR value.

Peak amplitude (pixels)	Quality Index	Validity
5-7	1	Y: representative of cardiac pulse
>7	0	N: probably referred to movement or variations of ambient light

Figure 3.4: Quality index evaluation of time intervals

It is possible to observe in fig.3.5(a) an example of the periods considered valid with respect to the entire duration of the video: on average, the periods of quality 1 have an average duration of no more than one minute. In fig. 3.5(b) , 3.5(c), an enlargement of quality periods 0 and 1 and corresponding amplitudes.

3.3.5 ROI selection

For each valid period of time, as shown in fig. 3.6, on the first frame of the video sequence a region of interest (ROI) of the infant's face is manually selected and parameterized analogously to the box described in section 3.3.1.

This region is usually the forehead or the cheek area in order to consider homogeneous vascularized areas of exposed skin tissue.

Since the oscillations in pixels' intensity I want to extract from the ROI have to be related to the cardiac pulse - in terms of blood-absorbed light - it is important that the same area of the exposed skin is present in the ROI box over time. Generally, this test is superflous, as any movements should have been identified in 3.3.4, but it

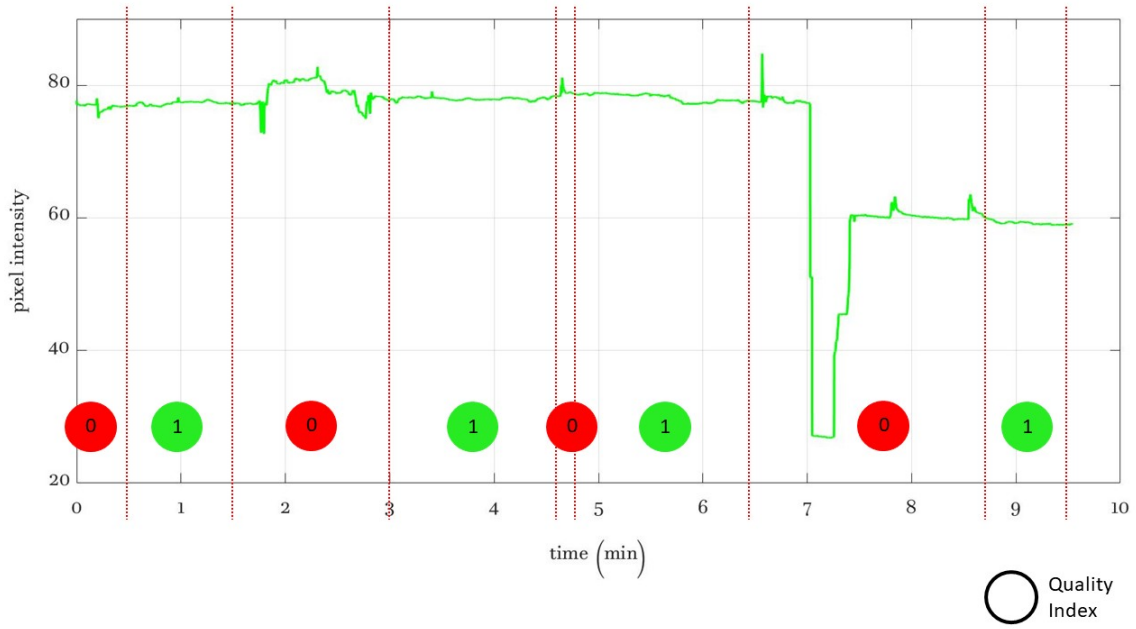

(a)

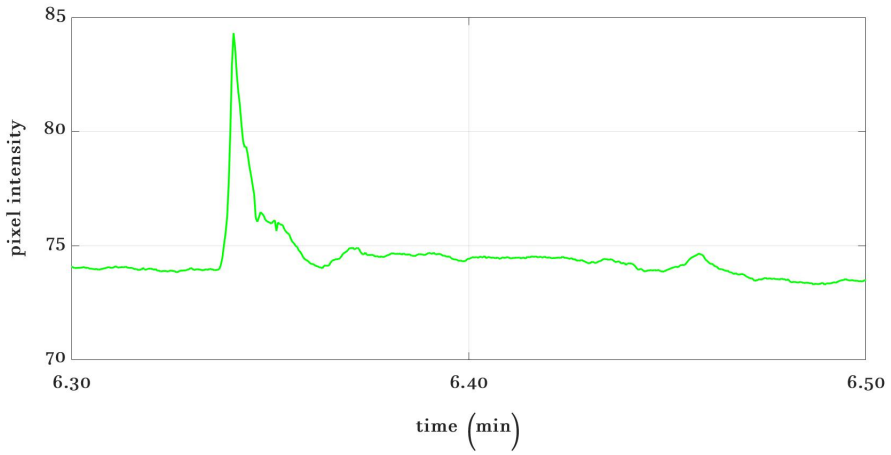

(b)

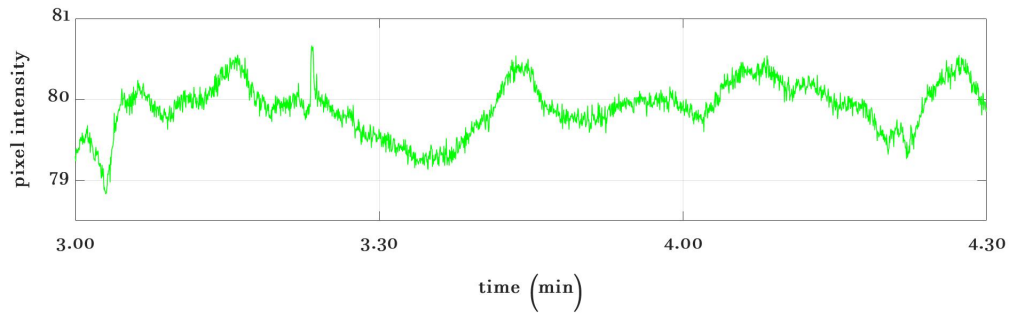

(c)

Figure 3.5: (detrended green trace, subject 7): (a) entire duration (b) detail min 6.5-6.7 (invalid) (c) detail min 3.0-4.30 (valid)

is still performed displaying the ROI every 15 seconds after 3.3.7 and, if necessary, redefined on the first frame.

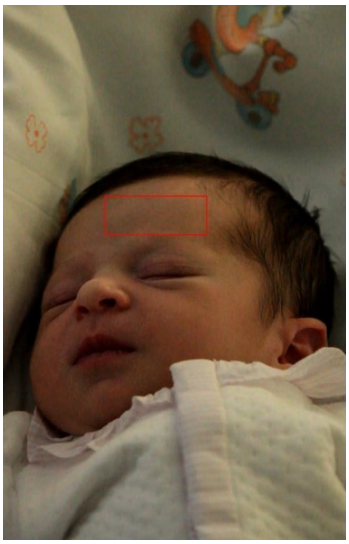

Figure 3.6: Example of selected ROI, subject 7

3.3.6 Averaging

This step, analogous to 3.3.2 , applied to green channel only and to periods considered valid, allows to extract a better ”raw” signal, since the information are derived only from the chosen region of interest (see an example in fig.3.7).

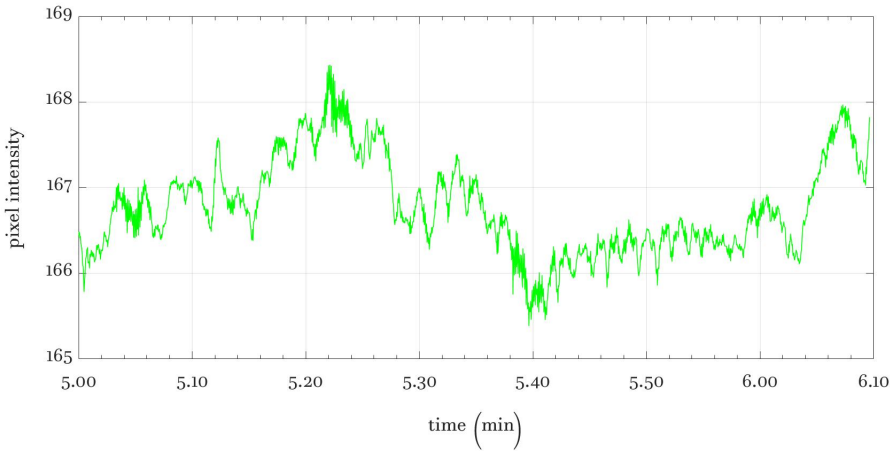

Figure 3.7: amplitude variations in green raw trace, subject 1

3.3.7 Detrending

As in 3.3.3, the continuous component (DC) of the "ROI obtained" signal is attenuated.

After this step, in the time domain, the signal results to start and end with values close to zero; in the frequency domain, it is instead possible to observe a strong attenuation of the components at very low frequencies, due to DC (see fig.3.8).

The signal representation in the frequency domain was obtained by Fast Fourier Transform (FFT): an algorithm optimized to calculate the discrete Fourier transform (DFT). More details on DFT are described in 3.3.10.

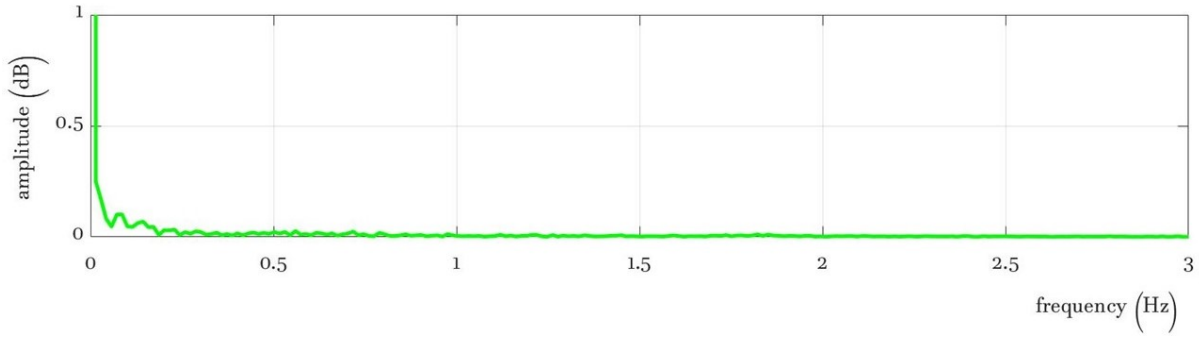

(a)

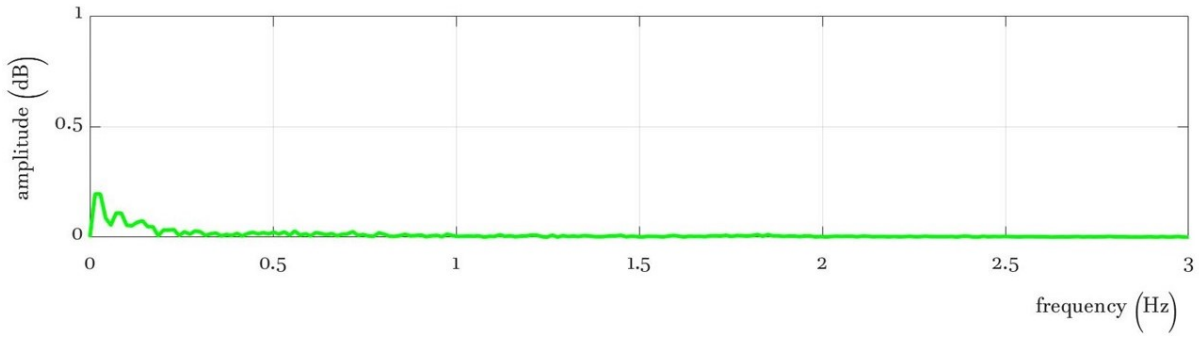

(b)

Figure 3.8: (signal spectrum, subject 1): (a) before detrending (b) after detrending

3.3.8 Data windowing

Since the heart rate is measured in beats per minute, I chose to process the signal by splitting it into windows lasting one minute submultiple: 15 seconds.

The running window slides on the signal every 2 second, corresponding to the sampling frequency of the reference pulse oximeter. This way, the following processing results to be sufficiently accurate.

I expect every 15-second window to present about 25-30 cardiac pulse, according to the physiological range of an healthy term infant.

3.3.9 Filtering

The obtained signal represents the plethysmographic curves (graphic recording of the volume variations of the vessels induced by the respective variations of the contained blood).

Since the goal of the HR estimation stage is to investigate the heart rate values, it is necessary to filter, in the frequency domain, all the power components referable to sources different from cardiac pulsation.

For newborns, a physiological range for the cardiac pulse is approximately from 100 to 160 bpm [1], so the signal is manually pass-band filtered at the corresponding cutting frequencies of [1.7 - 2.7]Hz: all components outside these frequencies are attenuated.

In fig. 3.9 it is evident the presence, outside the band of interest, of components of high amplitude, such as the ones related to the heartbeat are 'masked' in power.

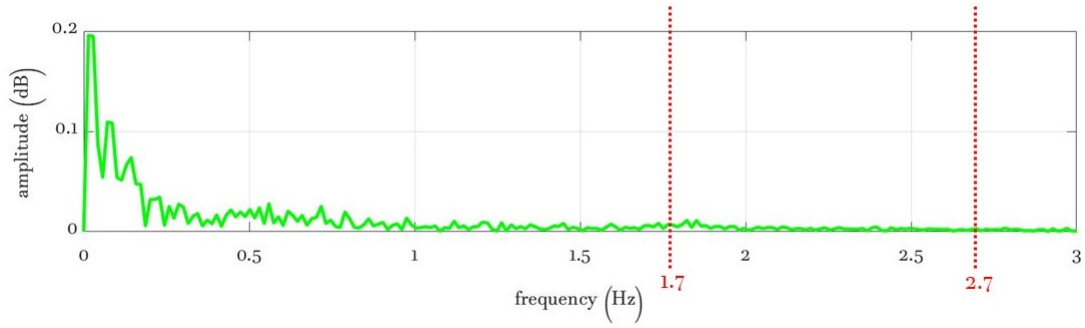

Figure 3.9: filtering cutoff frequencies (in red)

3.3.10 Spectral Analysis and HR Estimation

Finally, the spectrum of the signal in the frequency domain is estimated via the non-parametric technique of FFT with the aim of identifying the maximum peak, whose frequency corresponds, multiplied by 60 seconds, to the measurement of the heart rate in bpm (fig. 3.10).

The FFT method allows determining sufficiently accurate spectral estimates; the Fast Fourier Transform is an optimization of the Discrete Fourier Transform, a particular type of Fourier transform for finite sequences, as it is possible to consider the temporal windows in which the signal has been split.

To be consistent with the sampling performed by the reference sensor, the FFT is applied every two seconds on windows of 15 seconds (corresponding to about 375 samples due to the fr of 25fps).

To improve the performance, the FFT was represented on a number of points equal to the power of two whose exponent is the approximation (downwards) of the length of the signal expressed as power of two.

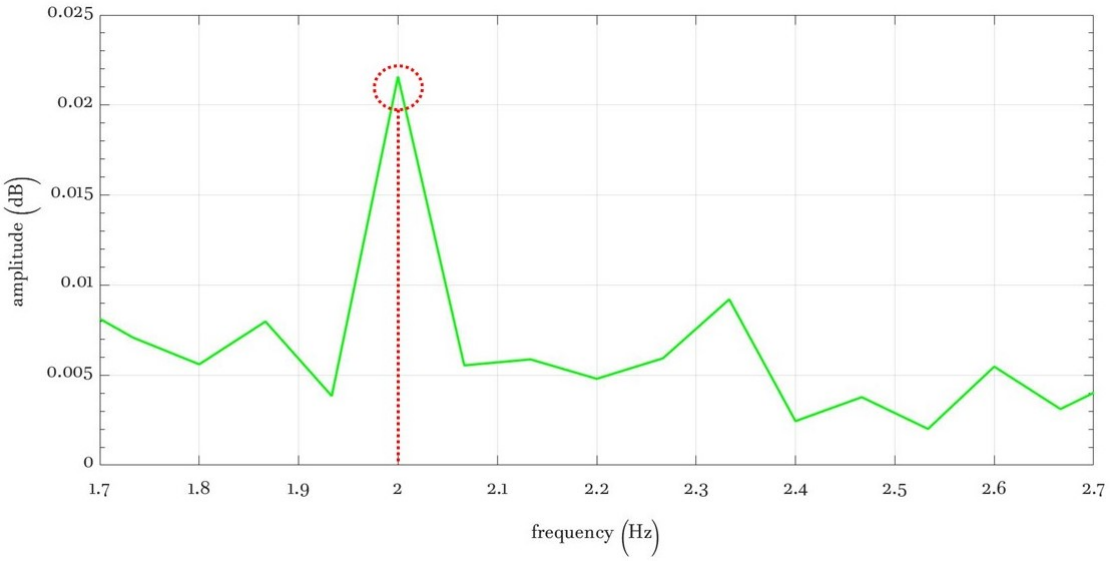

Figure 3.10: example of FFT, 15-second window, subject 7

Chapter 4

Setup

4.1 Instrumentation

The setting for acquisitions envisaged the use of:

- the clinical instrumentation used in practice for the measurement of HR and spO2 (Masimo Radical 7 Rainbow pulse oximeter, sw vs 1.1.48i) - see fig. 4.1(a)
- the Masimo MICT proprietary sw, vs 1.1.0.9 for the wired transmission (RS232 - USB 2.0) of the data (csv format) to the computer - see fig. 4.1(b)
- computer LENOVO IDEAPAD Y700-15ISK, Intel Core i7-6700HQ processor, CPU @ 2.60 GHz, 16 GB RAM, 64-bit operating system Windows 10 Home vs 1709
- Matlab R2016b to perform data processing

(a)

(b)

4.2 Reference signals

Masimo Radical 7 Rainbow pulse oximeter allows the recording and downloading of heart rate and blood oxygen saturation trends in CSV format using proprietary sw.

As can be seen from 4.1, the sampling rate is 2 seconds and both Sp02 and PR are logged into the file.

It is worth noting that the set of possible events is relatively large and this shows that the proposed architecture should run under different real conditions.

Alarms are activated in situations of (4.1); ranges referenced by the errors reported are expressed in (4.2, 4.3).

Moreover, some messages indicate configuration / arrangement errors of the device and of the sensor connected to it (4.4).

In table 4.1 an example of the downloadable format of data with reported alarms and messages.

MENU ITEMS	DESCRIPTION
SpO_2 HIGH LIMIT	The SpO_2 high alarm limit can be set anywhere between 2% and 99%, with a 1% step size. In the "----" (off) setting, the alarm can be turned off completely.
SpO_2 LOW LIMIT	The SpO_2 low alarm limit can be set anywhere between 1% and 99%, with a 1% step size. ***NOTE:*** *The low alarm limit always has to be set below the high alarm setting. When the high alarm limit is set below the low alarm limit, the low alarm limit will automatically adjust to the next setting below the newly entered high alarm limit setting.* ***NOTE:*** *The SpO_2 low limit can not be set below the password protected minimum low SpO_2 alarm limit. See Section 4, Operation, Display for details.*
PULSE RATE HIGH LIMIT (BPM)	The pulse rate high alarm limit can be set anywhere between 30 BPM and 240 BPM, with a 5 BPM step size.
PULSE RATE LOW LIMIT (BPM)	The pulse rate low alarm limit can be set anywhere between 25 BPM and 235 BPM, with a 5 BPM step size. ***NOTE:*** *The low alarm limit always has to be set below the high alarm setting. When the high alarm limit is set below the low alarm limit, the low alarm limit will automatically adjust to the next setting below the newly entered high alarm limit setting.*

Figure 4.1: possible reported alarms; source:*Masimo*

Table 4.1: example of downloaded data from Masimo Radical 7 PulseOximeter

DATE	TIME	SPO2	PR	...	Events
02/19/2018	16:17:06	100	138	...	
02/19/2018	16:17:08	100	137	...	
02/19/2018	16:17:10	98	135	...	
02/19/2018	16:17:12	95	129	...	QUALIFIED-ALARM-SPO2-LO
02/19/2018	16:17:14	90	129	...	QUALIFIED-ALARM-SPO2-LO
02/19/2018	16:17:16	87	75	...	QUALIFIED-ALARM-PR-LO

Figure 4.2: possible reported messages; source:*Masimo*

MESSAGE	POSSIBLE CAUSE(S)	RECOMMENDATION
AMBIENT LIGHT	• Too much light on patient (sensor). • Inadequate tissue covering sensor detector.	• Remove or reduce lighting. • Cover sensor from light. • Reposition sensor.
DEFECTIVE CABLE	• Oximeter cannot identify the connected cable or the cable has failed.	• Inoperative or faulty cable • Replace cable. • Refer to the Directions for Use of the cable being used.
INCOMPATIBLE SENSOR	• Not a proper Masimo sensor.	• Replace with a proper Masimo sensor. • Refer to Section 8.
INVALID SENSOR	• Oximeter cannot identify the connected sensor.	• Broken sensor cable wire or inoperative LEDs or faulty detector. • The sensor has failed. • Replace sensor. • Refer to the instructions for the sensor being used.
LOW BATTERY	• Battery charge is low.	• Charge battery by placing the Radical-7 Handheld into the Docking Station and powering the unit with AC line power. • Replace battery if necessary.
LOW PERFUSION	• Signal too small.	• Move sensor to better perfused site. • Refer to Section 4, *Low Perfusion.*
LOW SIGNAL IQ	• Low signal quality.	• Ensure proper sensor application. • Move sensor to a better perfused site. • Refer to Section 4, *Signal IQ.*
LOW SpCO CONF	• SpCO measurement reading is obscured.	• Ensure proper sensor application. • Check sensor to see if it is working properly. • If not, replace the sensor.
LOW SpMet CONF	• SpMet measurement reading is obscured.	• Ensure proper sensor application. Check sensor to see if it is working properly. • If not, replace the sensor
SPEAKER FAILURE	• Unit requires service	• Contact Masimo Tech Support. • Refer to Section 9 *Service and repair.*
NO CABLE	• Cable not attached or not fully inserted into the connector.	• Disconnect and reconnect cable into connector.

MESSAGE	POSSIBLE CAUSE(S)	RECOMMENDATION
NO SENSOR	• Sensor not fully inserted into the connector.	• Maybe an incorrect sensor, or a defective sensor or cable. • Insert sensor into connector. • Disconnect and reconnect sensor. • Refer to the instructions for the sensor being used.
	• Unit is searching for patient's pulse.	• Disconnect and reconnect the sensor into the Patient Cable Connector.
PULSE SEARCH	• Unit is searching for patient's pulse.	• If values are not displayed within 30 seconds, disconnect and reconnect sensor. • If pulse search continues, remove sensor and replace on a better perfused site.
SENSOR CALIBRATING	• Unit is checking the sensor for proper functioning and performance.	• If values are not displayed within 30 seconds, disconnect and reconnect sensor. • If values are still not displayed, replace with a new sensor.
SENSOR OFF	• Sensor off patient.	• Disconnect and reconnect sensor. • Reattach sensor.
SERVICE REQUIRED*	• Internal Failure.	• Unit requires service.
UNRECOGNIZED CABLE	• Not a proper cable.	• Replace with a proper cable. Refer to Section 8.

Figure 4.3: possible reported messages; source:*Masimo*

TYPES	SpO_2 (HIGH)	SpO_2 (LOW)	PULSE RATE (HIGH)	PULSE RATE (LOW)
ADULT LIMITS†	Off	90%	140 BPM	50 BPM
NEONATAL LIMITS†	100%	90%	180 BPM	100 BPM
CUSTOM LIMITS*	Off*	90%*	140 BPM*	50 BPM*

Figure 4.4: tolerated range; source:*Masimo*

4.3 Video recording

Two sets of videos have been adopted to test the efficiency of the proposed architecture: a first time using the **Axis M1034-W NETWORK camera** (4.2) - mounted at the end of a specially designed arms - then using the **Canon EOS 600D SLR**, manually configured according to the necessary exposure times and ISO parameters (4.3).

Table 4.2: General features and specification for the for the Axis M1034-W NETWORK camera. (Source: Axis)

Item	Description
Imaging Sensor	1/4” progressive scan RGB CMOS
Image size (pixels)	1080 (H) x 800 (W)
Max frame rate	25/30 FPS
Video Data Output	24-bit digital data
Gain & Exposure	Automatic/Manual

Table 4.3: General features and specification for the for the Canon EOS 600D camera. (Source: Canon)

Item	Description
Imaging Sensor	22,3 x 14,9 mm CMOS
Image size (pixels)	1080 (H) x 1980 (W) Full HD
Actual Pixels	18 Mpixels
Total Pixels	18,7 Mpixels
Sensor Ratio	3:2 Max frame rate
50 FPS	
Max recording time	13 minutes (at the current resolution)
Video Data Output	24-bit digital data
Gain & Exposure	Automatic/Manual

4.4 Time synchronisation

Before conducting the experimentation, all the devices were configured with the same date and time in UTC / GMT +1 format.

The recordings are always started a few minutes after attaching the sensor to the baby's foot, so as not to consider the transient in which the sensor stabilizes.

Timestamps were used to synchronise downloaded data from Masimo software and stored videos in Matlab.

4.5 Best Conditions

During the experimentation, various lighting conditions, positioning and configuration of the cameras, positioning of the device and the sensor were tested. Following the experiences made, it emerged that the best conditions for making registrations are:

- Light Source
  - ambient light as the only source of illumination (artificial light introduces components that must be corrected during post-processing)
  - the light source must flood the subject's face, in particular the forehead area, in the most uniform way possible (avoid placing objects between the source and the face that can project shadows)
- Photoreceptor
  - camera positioned frontally with respect to the subject at a distance of no more than 1m, 1.5m; possibly on a stable support so as not to introduce unwanted micromovements
  - a constant frame rate, preferably 25 fps
  - manual white balance settings and ISO values so that they are the same intra-video and inter-video
  - autofocus off so as not to change the distance of the lens from the subject
  - RGB video color coding
  - the videos were acquired at a resolution of, but lower resolutions showed good results anyway
  - a minimum duration of at least 10 minutes guarantees in most cases to be able to identify at least some valid period of analysis if the algorithm does not provide for the implementation of compensation of motion artifacts

- Pulse-oximeter
  - requesting the sw to download the reference data simplifies the comparison of digital data
  - positioning the device inside the shot allows you to easily synchronize data by viewing the display directly in the video
  - it can be useful, especially for long monitoring, to keep the device in charge: in the specific case of the Masimo Rainbow, the performance in the case of *low-battery* may be less accurate
  - it is also always good to wait a few minutes after positioning the sensor before starting monitoring: pulse oximeters generally have a minimum transient period to stabilize

Chapter 5

Clinical Study Design

5.1 Introduction

The experimentation was carried out between November and May 2018 in the changing room of the pediatric and neonatal ward of the Mauriziano hospital in Turin.

A total of ten newborns were taken into account during recording sessions of about ten consecutive minutes per child.

The camera was mounted in order to frame child face and chest in a frontal manner and at the same time during the months (fig. 5.1); since it is a first study, the most favorable conditions were chosen (ambient light only) and more easily repeatable (same positioning of the cradle, same position of the camera, same recording times).

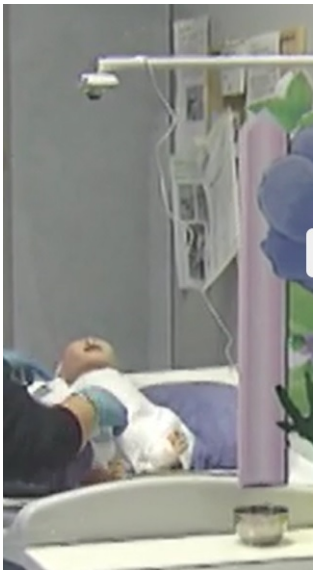

Figure 5.1: example of acquisition setup

5.2 Patient Population

Patients were selected from newborns whose families consented to the research.

The study involved ten healthy children of both sexes, of a gestational age ranging from 36 to 41 weeks (born pre-term or at term), of different ethnicity provided they had a skin color considered 'fair-skinned'.

Recordings were acquired in the nursery changing room in moments of regular staying or during spontaneous sleep, without interfering with the normal activities of the hospital or with the visiting hours of the families, and without any health implication for the subject.

Ten healthy newborn babies were tracked, gestational age ranging from 36 to 41 weeks (see fig. 5.2).

Subject	Gender	Gestation Period (weeks)
1	M	39
2	F	41
3	M	40
4	M	37
5	F	36
6	M	38
7	F	40
8	M	40
9	F	36
10	M	39

Figure 5.2: Patients Caractheristichs

5.3 Informed Consent and Privacy

For the acquisition of newborn recordings, the documentation relating to the clinical study protocol was drafted and approved by the Local Ethic Committee of the Mauriziano Hospital (Turin, Italy).

Families of each newborn have signed a form giving informed consent to videotaping and the baby's participation in the experimentation as described and a note on data privacy according to the updated provisions and supplemented by Italian legislative law 196/2003.

5.4 Recording Sessions

The recording sessions were organized so as not to interfere with the visiting hours of parents or with the usual clinical practices.

Each infant was accompanied and assisted in the changing room by the hospital's medical staff and parents were allowed, if required, to attend the sessions from outside.

All the children were assisted, during recordings, by a pediatrician who also measured the respiratory rate regularly at 5-minute intervals.

During the first session of recordings, a bradycardia event was detected in a subject, noticed by a lowering of the heart rate around 80 bpm and an associated decrease in oxygen saturation; in this case the pediatrician reported the event and further investigations were carried out.
This is just one of the examples that show the importance of the test and screening sessions planned for all newborns, even in good health: the monitoring of vital parameters assisted by specialized doctors during the first days of life is essential to detect any anomalies that are difficult to identify by means of only medical examination.

The use of completely contactless methods in monitoring and screening sessions (if they guarantee an acceptable measurement accuracy), facilitates a possible intervention of the doctors in case of anomalies, which must not detach sensors and wires; benefits are even more appreciable in intensive care, where monitoring is continuous.

Chapter 6

Experimental Results

6.1 Dataset

As previously mentioned, data sets have been acquired with two different cameras: the results presented will relate to the acquisitions made with the **Canon EOS 600D SLR**, as they provide better performances.

One of the main reasons that justify the choice is the need to work with recordings at a constant frame rate.

Since the heart rate is measured in beats per minute and the video starting signal is a sequence of values (average of the pixels) corresponding to each frame, we need to know how many samples (frames) correspond to one second and then to one minute.

As an IP camera, the **Axis** provides bandwidth-dependent performance, and there has also been a noticeable change in frame rate during recording that is highly dependent on ambient brightness.

6.2 Comparison Plots

A first method to evaluate the accuracy of the results obtained with respect to the ground-truth has been plotting the two series in the same figure.

To the eye, the eventual difference in terms of bpm is immediately evident and moreover, very important from the clinical point of view, it is noticeable how effectively the series of estimated values follow the reference trend.

It is important to distinguish two different situations, in which a different accuracy could be observed: cases in which the HR values remain relatively constant over time (6.1 , 6.2) and cases in which there are more sensitive variations in HR serie (6.4 , 6.3).

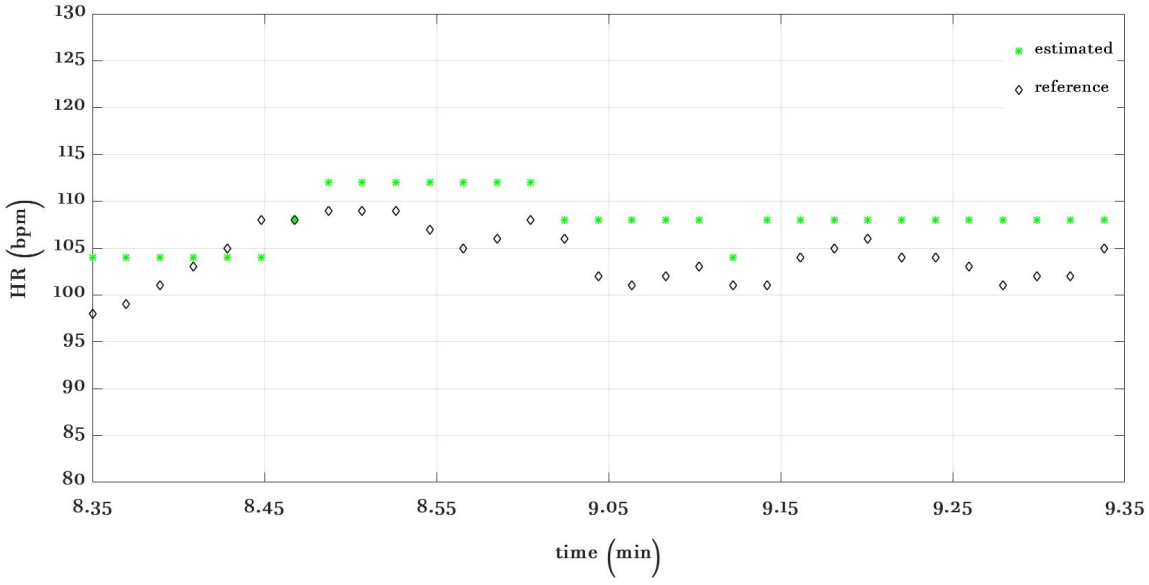

Figure 6.1: Example of constant HR compared results, Subject 1: * estimated, : reference

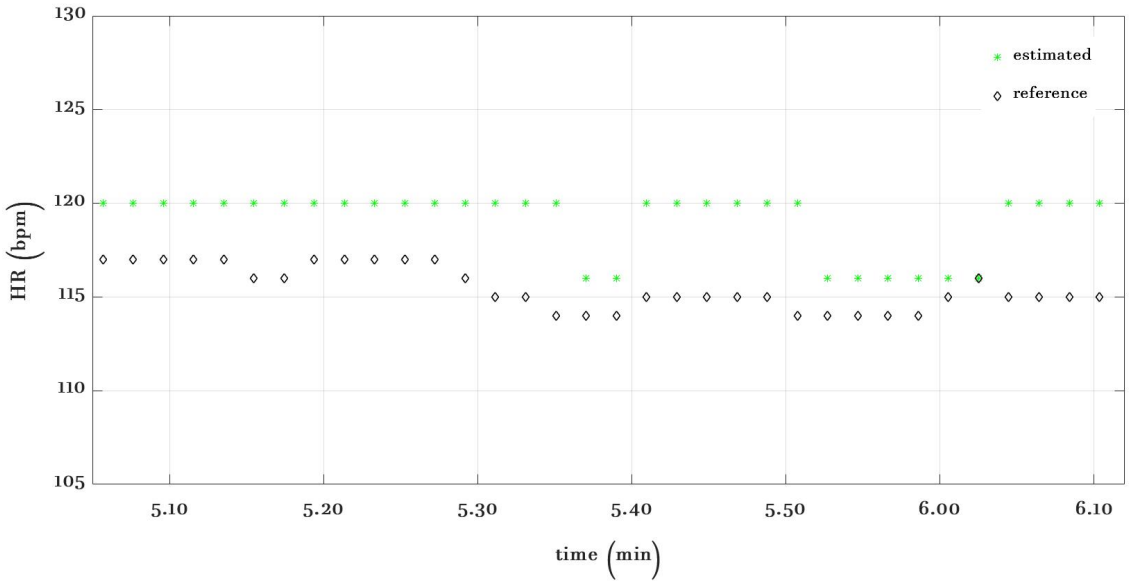

Figure 6.2: Example of constant HR compared results, Subject 7: * estimated, : reference

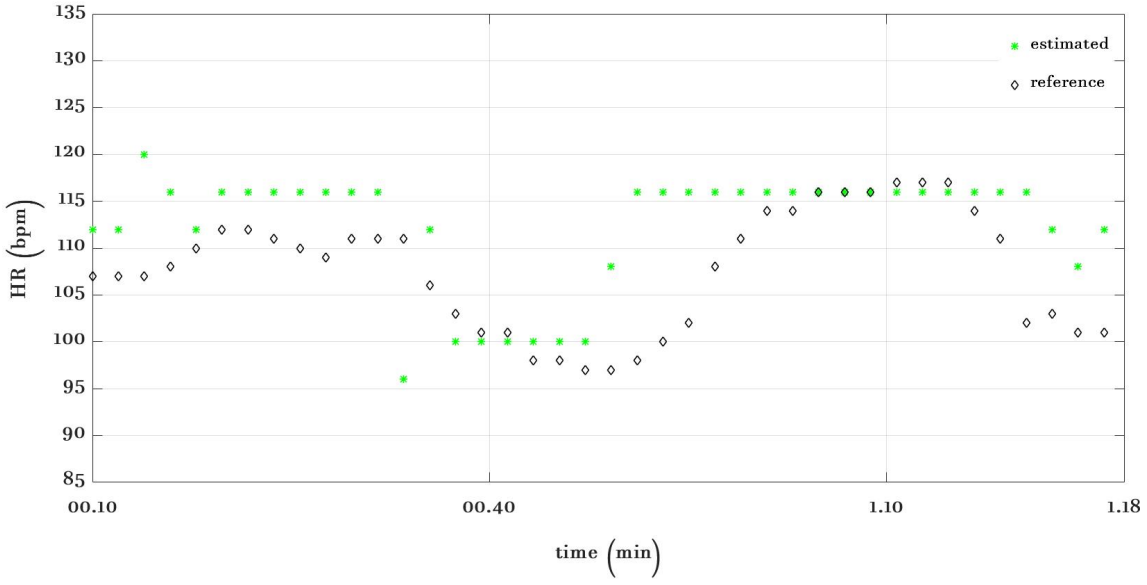

Figure 6.3: Example of variable HR compared results, Subject 8: * estimated, : reference

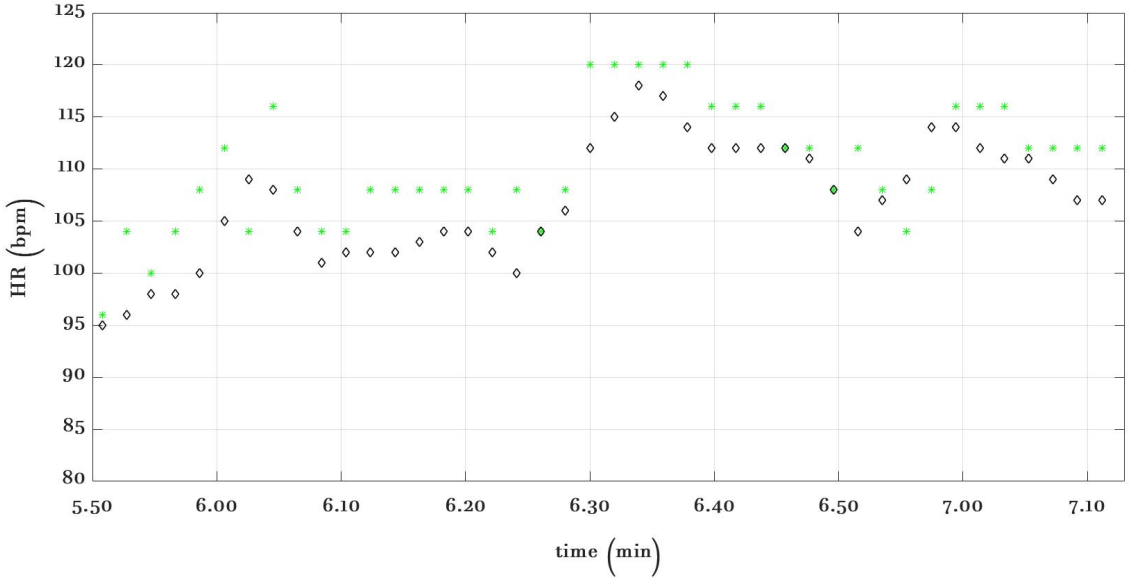

Figure 6.4: Example of variable HR compared results, Subject 2: * estimated, : reference

Some considerations: in infants it is physiological to observe a generally high cardiac variability, but it must be taken into account that the patients of the present trial were monitored in wakefulness or spontaneous sleep, situations in which no particularly high variations are expected, as it may be expected for example during a painful event.

It is therefore likely that sensitive variations may be due to particular physiological events (such as crying or regurgitation) or to movements of the newborn during recording, with the possible consequences: lower accuracy of the measure, already at the level of ground-truth (the Masimo device guarantees an accuracy of ±5 bpm in the case of movement against ±3 bpm in case of non-movement) or even cause a detachment of the sensor, reported in downloaded data by the *sensor_off_patient* error and which has been taken into account in the evaluation of the validity of the signal.

So generally, in this work, the greater the oscillations in bpm, the lower is the accuracy of the estimate expected. However, the following analysis show an acceptable accuracy of estimates in both cases.

For each valid period of every subject, the absolute error was calculated as:

$$|(estimated - reference)| \tag{6.1}$$

then, the mean and standard deviation of this difference vectors were calculated.

Below, the tables (6.6 , 6.7 , 6.8 , 6.9 , 6.10 , 6.11 , 6.12 , 6.13 , 6.14 , 6.15) with the values corresponding to the videos of each patient (valid periods only) are reported. Among the represented parameters, the Pearson coefficient r is also indicated: a linear correlation index between data sets (fig. 6.5) also useful for the subsequent analysis and linear representation of data using the Bland-Altman method.

Pearson coeff *r*	correlation
1	linearly matching data sets
0	no linear correlation

Figure 6.5: Pearson's coefficient ends

valid period (min)	abs error : mean (bpm)	abs error: st. deviation (bpm)	Pearson Coefficient
1.00 – 2.09	4,18	2,68	0,67
2.35 – 4.00	3,14	2,01	0,69
5.00 – 6.10	3,46	2,36	0,75
6.37 – 8.00	3,5	1,58	0,82
8.35 – 9.55	4,15	1,89	0,61
11.50 -	5,36	4,25	0,79
(mean value) →	4	2	0,72

Figure 6.6: subject 1: parameters and values relating to valid recording periods

valid period (min)	abs error : mean (bpm)	abs error: st. deviation (bpm)	Pearson Coefficient
0.00 – 1.20	5,39	3,96	0,71
5.30 – 7.20	5,20	1,7	0,85
(mean value) →	5	6	0,78

Figure 6.7: subject 2: parameters and values relating to valid recording periods

valid period (min)	abs error : mean (bpm)	abs error: st. deviation (bpm)	Pearson Coefficient
3.00 – 4.25	3,68	2,43	0,63
8.43 – 10.43	4,27	1,75	0,70
(mean value) →	4	2	0,66

Figure 6.8: subject 3: parameters and values relating to valid recording periods

valid period (min)	abs error : mean (bpm)	abs error: st. deviation (bpm)	Pearson Coefficient
0.23 – 1.36	4,94	2,84	0,86
2.41 – 3.30	4,15	2,54	0,65
4.52 – 5.45	4,8	2,68	0,88
8.20 – 9.26	3,67	1,37	0,77
(mean value) →	4	2	0,79

Figure 6.9: subject 4: parameters and values relating to valid recording periods

valid period (min)	abs error : mean (bpm)	abs error: st. deviation (bpm)	Pearson Coefficient
no valid periods were found (crying baby, continuous movements, hands in front of the face)			

Figure 6.10: subject 5: no valid periods, some examples discussed in 6.5

valid period (min)	abs error : mean (bpm)	abs error: st. deviation (bpm)	Pearson Coefficient
0.06 – 2.47	3,42	2,23	0,73
5.35 – 7.20	3,59	4,6	0,68
(mean value) →	3	3	0,71

Figure 6.11: subject 6: parameters and values relating to valid recording periods

valid period (min)	abs error : mean (bpm)	abs error: st. deviation (bpm)	Pearson Coefficient
00.15 – 1.30	3,97	1,47	0,61
3.00 – 4.30	4,37	1,72	0,56
4.50 – 6.30	3,81	1,60	0,72
8.47 – 9.32	4,60	0,63	0,92
(mean value) →	4	1	0,70

Figure 6.12: subject 7: parameters and values relating to valid recording periods; in green, the r value of the highest correlation of the experimentation, see more details in 6.4

.

valid period (min)	abs error : mean (bpm)	abs error: st. deviation (bpm)	Pearson Coefficient
0.10 – 1.45	5,72	4,89	0,56
2.00 – 2.30	4,75	3,28	0,73
2.45 – 4.36	5,81	3,23	0,82
5.10 – 6.00	4,17	2,23	0,49
(mean value) →	5	3	0,65

Figure 6.13: subject 8: parameters and values relating to valid recording periods; in red, the r value of the lowest correlation of the experimentation, see more details in 6.4

valid period (min)	abs error : mean (bpm)	abs error: st. deviation (bpm)	Pearson Coefficient
1.03 – 1.50	8,37	4,59	0,59
2.37 – 3.37	3,6	1,75	0,91
3.50 – 5.38	4,02	2,17	0,67
(mean value) →	5	3	0,73

Figure 6.14: subject 9: parameters and values relating to valid recording periods

valid period (min)	abs error : mean (bpm)	abs error: st. deviation (bpm)	Pearson Coefficient
0.13 – 1.45	5,34	2,78	0,68
2.20 – 3.35	6,15	3,49	0,71
4.00 – 4.36	4,22	4,21	0,76
5.25 – 6.37	5	2,75	0,73
8.00 – 9.10	3,91	4,1	0,84
(mean value) →	5	3	0,74

Figure 6.15: subject 10: parameters and values relating to valid recording periods

6.3 The Bland-Altman analysis

It was chosen to report the comparison between estimated and ground-truth values through Bland-Altman analysis and representation [22].

In the first plot of Bland Altman (fig. 6.16), the x axis represents the HR values measured by the pulse oximeter, the y axis instead, represents the difference between estimated values and reference values.

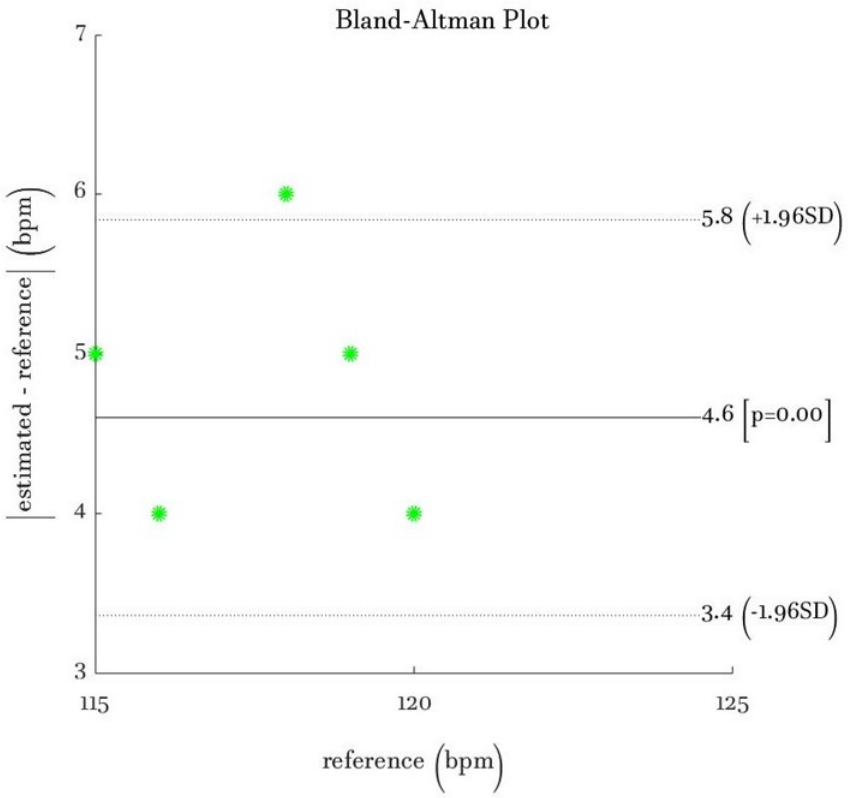

Figure 6.16: Bland-Altman plot subject 7: absolute error (difference) on y axis, reference data on x axis

The two statistical parameters of *mean* and *standard deviation* (SD) of the differences are calculated.

Generally, in a clinical setting, data sets are considered to be comparable if the dispersion of differences (green points) is included in the range

$$[mean \pm (1.96 * SD)] \tag{6.2}$$

In this case, on average, the difference between the estimated values and the reference is equal to 4.6 bpm.

Furthermore, it can be deduced that for reference values between [115-117] and [119-125] bpm, the implemented algorithm overestimates or underestimates about 4-5 bpm, while when the reference measures 118 pbm, the error is 6 bpm.

From fig. 6.17 further information are deduced: by representing on the y axis the estimated data, it is possible to evaluate to the eye the degree of correlation between the two measurements; the values are close to the continuous line, offset by an amount equal to the mean of the differences (4.6 bpm) compared to the ideal case (dotted line).

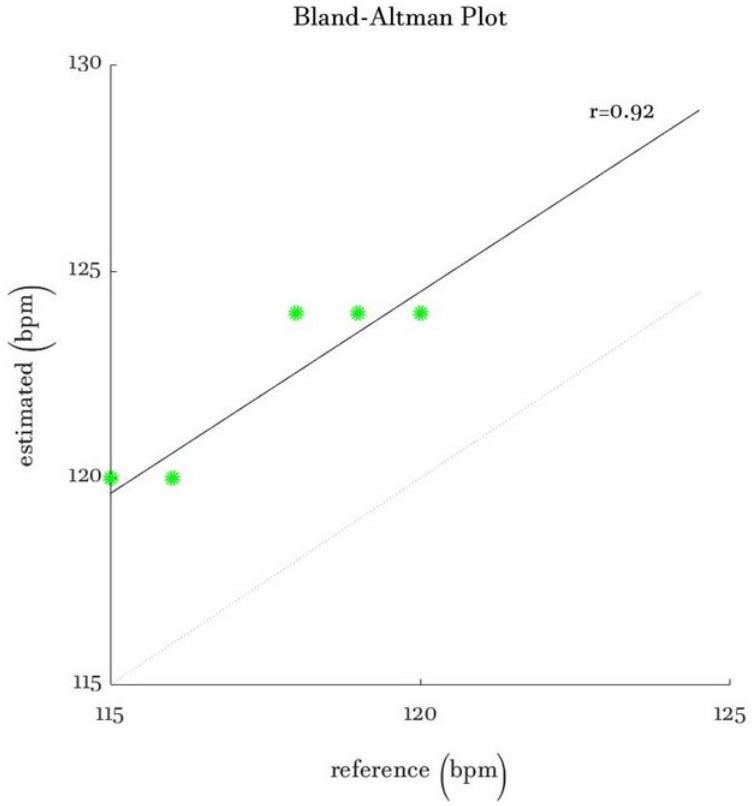

Figure 6.17: Bland-Altman plot subject 7: estimated on y axis, reference data on x axis

The tolerance limits were also established based on the accuracy of the reference instrument used (fig. 6.18).

The analysis of Bland-Altman thus allows to highlight, in the second plot, the degree of linear correlation between the two sets of data and its dispersion independently of the absolute error, a very important aspect that, if not detailed, can lead to deviant conclusions.

Saturation Accuracy		Pulse Rate Accuracy	
No Motion	Motion	No Motion	Motion
± 2%	± 3%	± 3 bpm	± 5 bpm
± 2%	± 3%	± 3 bpm	± 5 bpm

Figure 6.18: Masimo sensors accuracy

6.4 Discussion

6.4.1 Specific video

Three values have been reported in the results tables:

- in fig. 6.13, a low correlation is indicated by the Pearson coefficient equal to 0.49: observing the other parameters, it's possible to note an associated average absolute error equal to about 4 beats per minute, lower than that of the subject 7 -fig. 6.12 - (about 5 bpm) which instead shows a coefficient of corresponding correlation very high (0.92).
  This is an indication of the fact that, based only on the average value of the absolute error, it is not possible to actually establish whether a small difference between the values of the two series necessarily corresponds to their good correlation.
  Fig. 6.19 shows the plot of Bland-Altman for subject 8 - fourth valid period - : most of the points are dispersed away from the diagonal dashed of the 'ideal' correlation, unlike what is instead for the subject 7 (fig. 6.17).

- in fig. 6.14 the high average absolute error value during the first valid period is highlighted, subject 9: observing the video it was possible to detect micromovements of the camera, which introduced variations not attributable to the cardiac pulse but at the same time not so high and therefore detectable in the analysis of the validity based on amplitude threshold.

  This result suggests the implementation of a validity analysis method based on the tracking of some points of the face, in order to follow any movements of the face during the shooting, due to the subject or, in this case, to a non-stabilization of the camera.

For all valid periods analyzed, the Bland-Altman plot confirms the comparability between estimate and reference, with a concentration of points included in the range 6.2. Some examples below: 6.20, 6.21, 6.22, 6.23.

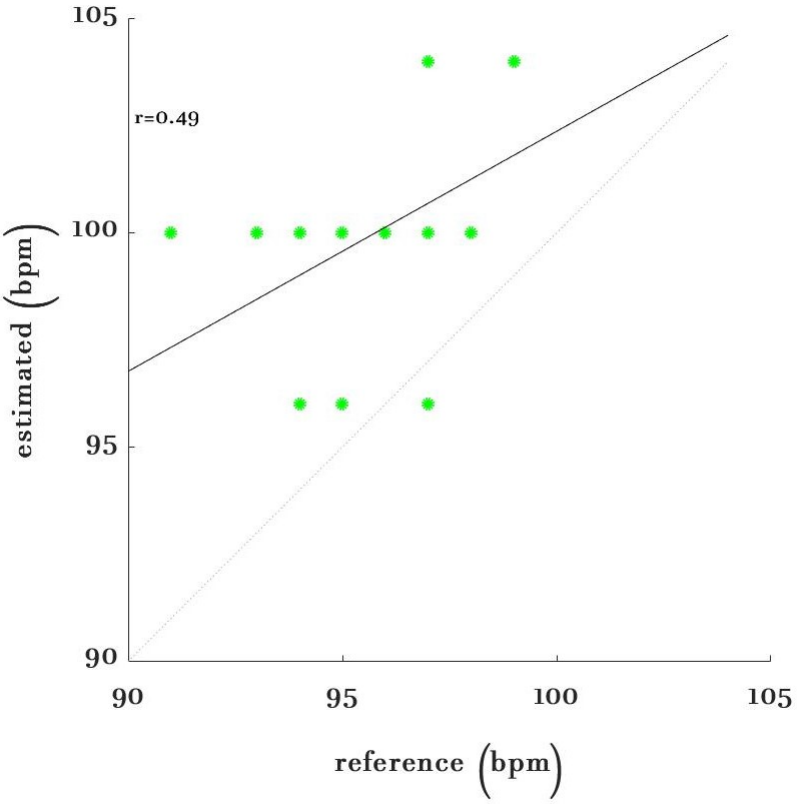

Figure 6.19: Bland-Altman linear plot, subject 8

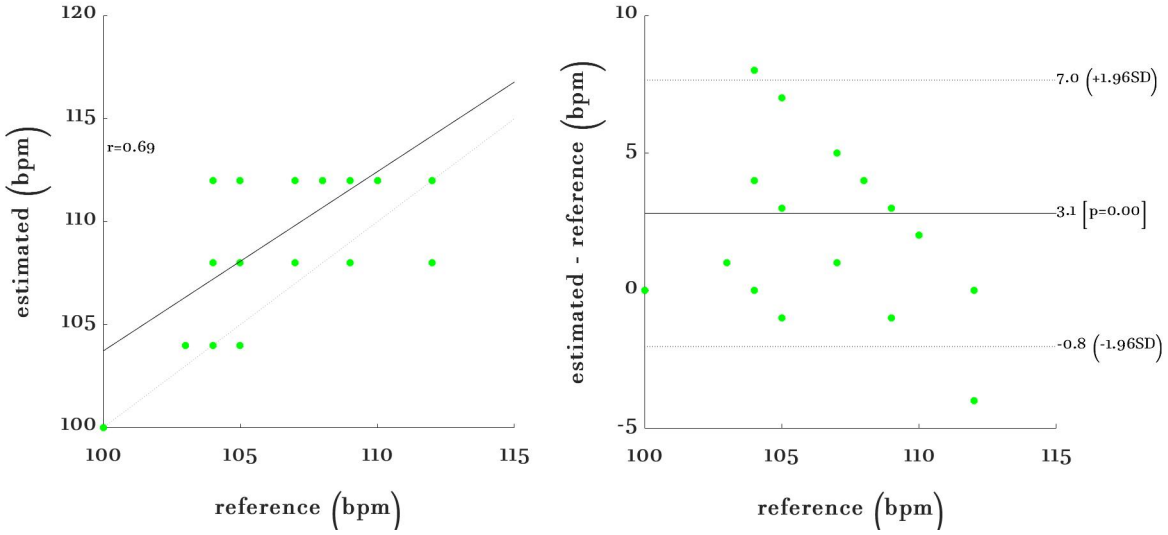

Figure 6.20: Bland-Altman plots, subject 1 valid period 2

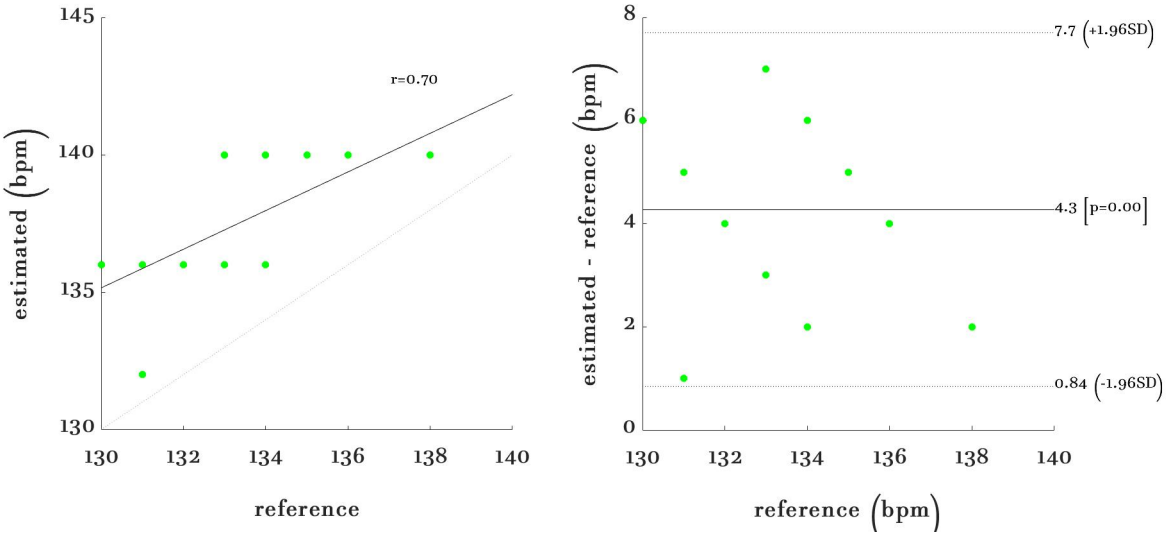

Figure 6.21: Bland-Altman plots, subject 3 valid period 2

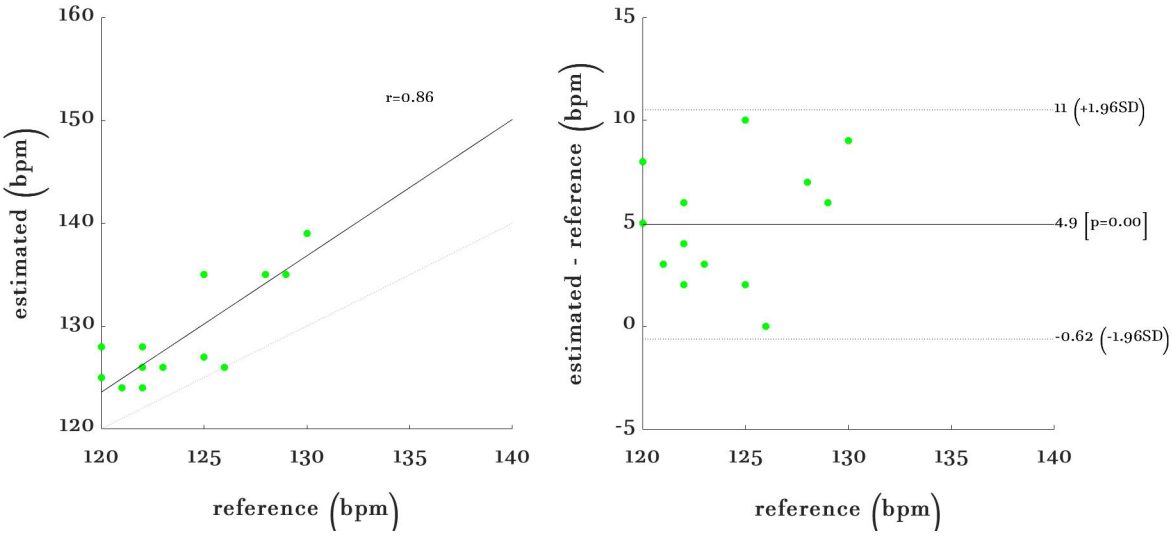

Figure 6.22: Bland-Altman plots, subject 4 valid period 1

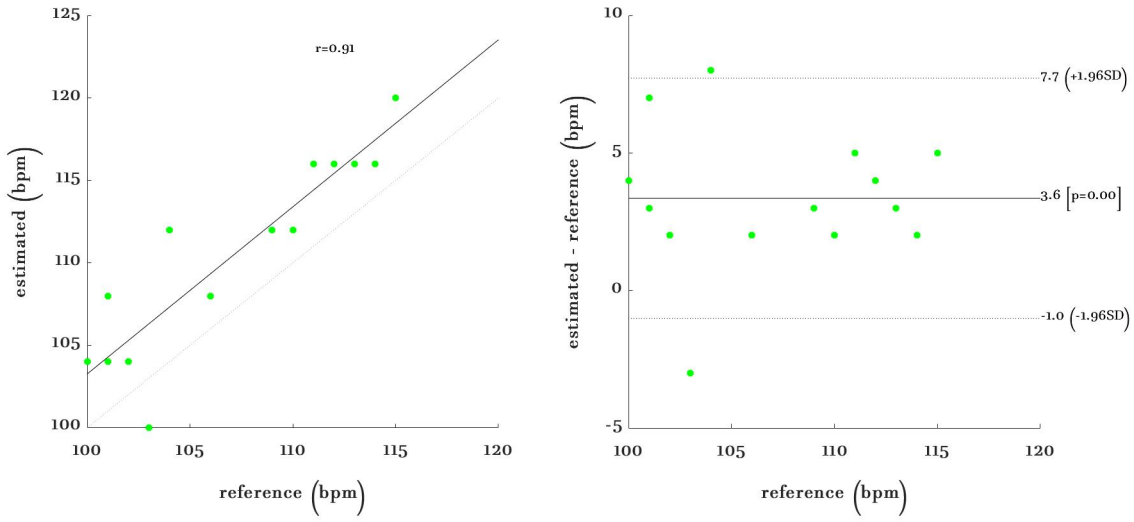

Figure 6.23: Bland-Altman plots, subject 9 valid period 2

6.4.2 Entire dataset

It is noted that on all the videos, in the periods of time considered valid, the estimate of the HR value differs on average by 4 bpm with respect to the reference value. This is a very encouraging result, if we think that the reference device has an accuracy, in the case of non-movement, of 3 bpm.

Moreover, it is possible to appreciate a correlation coefficient (Pearson) equal to 0.72 on average, an indication of a good correlation between the data sets and therefore an expression of the fact that the estimates are able to follow the trend of physiological variation.

It is therefore possible to consider promising the proposed method, with some reservations suggesting future developments.

By analyzing the method extended to the entire data set, one particular limitation of the implemented method is highlighted.

Figure 6.24 shows the percentage of valid signal used compared to the entire duration of the recordings: in most cases, the ”saved” periods make up less than half of the video material available, because the method implemented is an adaptation to what has been experimented so far in adults - which can be asked to remain relatively still and frontal compared to a video camera - and, especially in the case of experiments carried out on volunteers, it is possible to design rooms in controlled light conditions.

By shifting the focus on newborns, the method is applied to patients subject to frequent movement (the maximum duration of validity periods is shown, corresponding to 2.41 minutes and an average of 1.30 minutes) and in a clinical environment in

Subject	Valid signal (% respect to entire)	Valid signal (period of maximum duration)
1	75 %	1.25 min
2	32 %	1.50 min
3	34 %	2.00 min
4	40 %	1.13 min
5	0 %	0 min
6	44 %	2.41 min
7	31 %	1.40 min
8	28 %	1.51 min
9	28 %	1.48 min
10	58 %	1.32 min
Mean value →	37 %	1.36 min

Figure 6.24: dataset analysis

which ambient light varies in non-negotiable way, nor is it easy to avoid shadows due, for example, to the passage of medical personnel in the ward.

As already reported in the chapter "Literature Review", section "State of the art", some solutions have been proposed, but a more in-depth discussion is referred to the chapter "Conclusions".

6.5 Examples of "invalid periods"

In this section, two examples of the results obtained on periods considered invalid are presented.

6.5.1 Motion

In this first example it's possible to observe what we get when the baby moves during the recording: in fig. 6.25 a plot of the frame and the box of the identified face. The time window reported (a plot every 5 seconds) shows how the presence of the pacifier, the movement of the baby's head and at some point the movement of the hands in front of the face, affect the amount of light reflected and the shadows that come to create, helping to vary the average pixel value in the selected area over time.

In figure 6.26 it is evident how in a short time the intensity of the pixels varies in a width of range of about 20 pixels, against 5-7 which is generally expected for oscillations due to the pulse rate alone.

In figure 6.27, the flattening of the signal due to the detrending step is observed, but on 15-second windows the oscillations continue to vary with amplitudes around 10 pixels, still greater than 7, threshold set for validity.

The accuracy of the method in these situations is very low, as demonstrated by the results in fig. 6.28 and by the analysis of Bland-Altman (6.29): the estimated data are very far from those of reference, with a Pearson linear correlation coefficient of just 0.17.

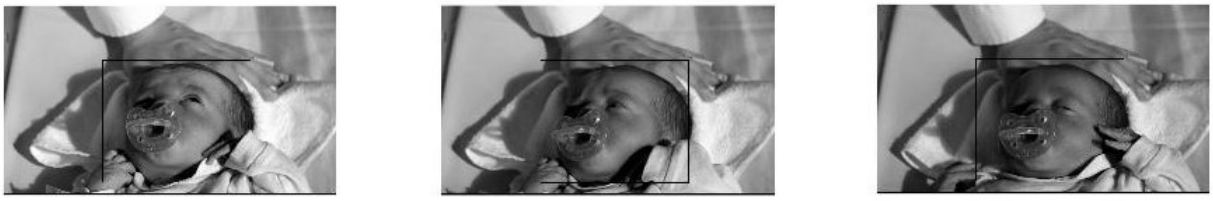

Figure 6.25: subject 5, frame plot every 5 seconds: it’s possible to observe baby movements

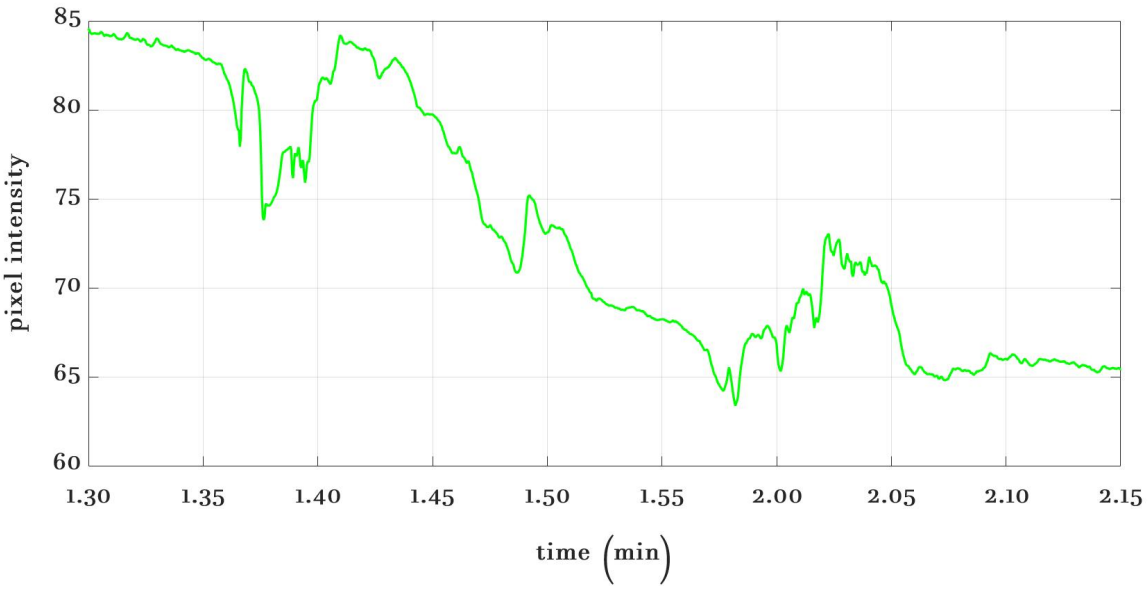

Figure 6.26: subject 5; raw trace obtained averaging frame pixels

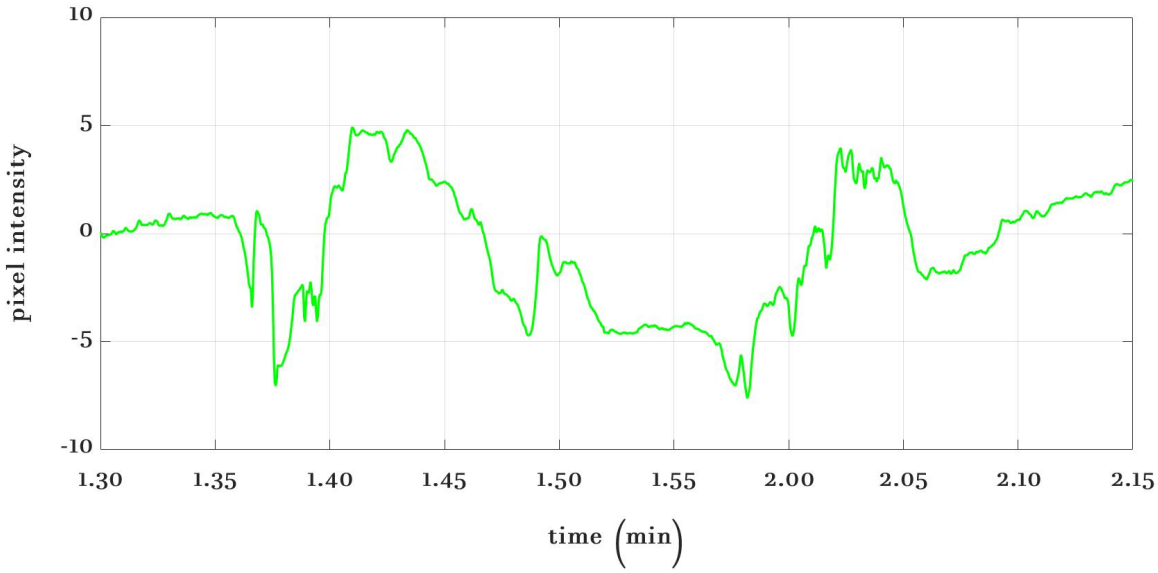

Figure 6.27: subject 5; detrended trace

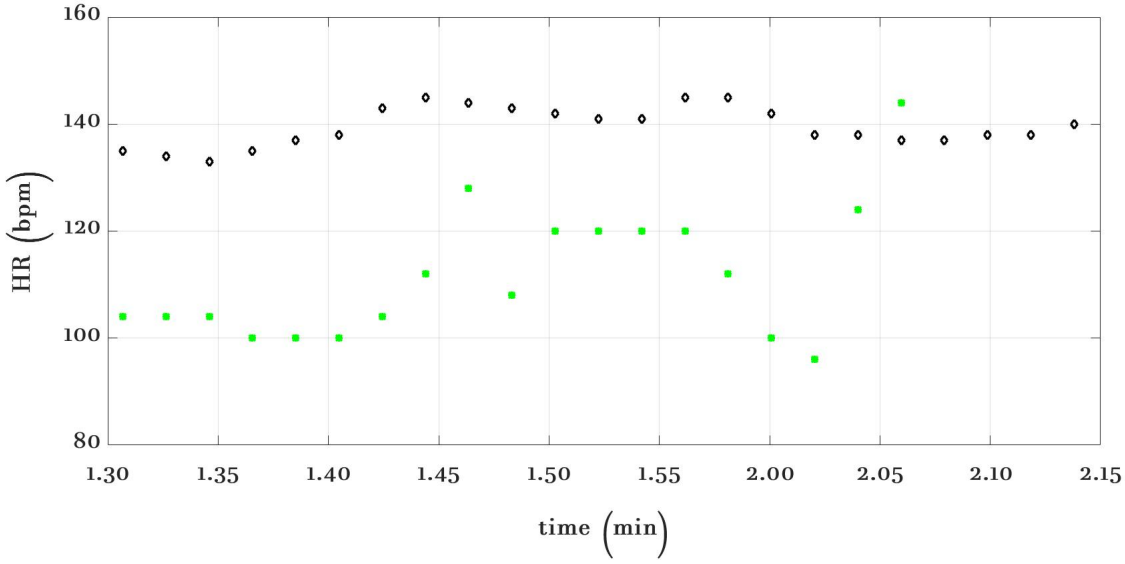

Figure 6.28: subject 5; HR results comparison

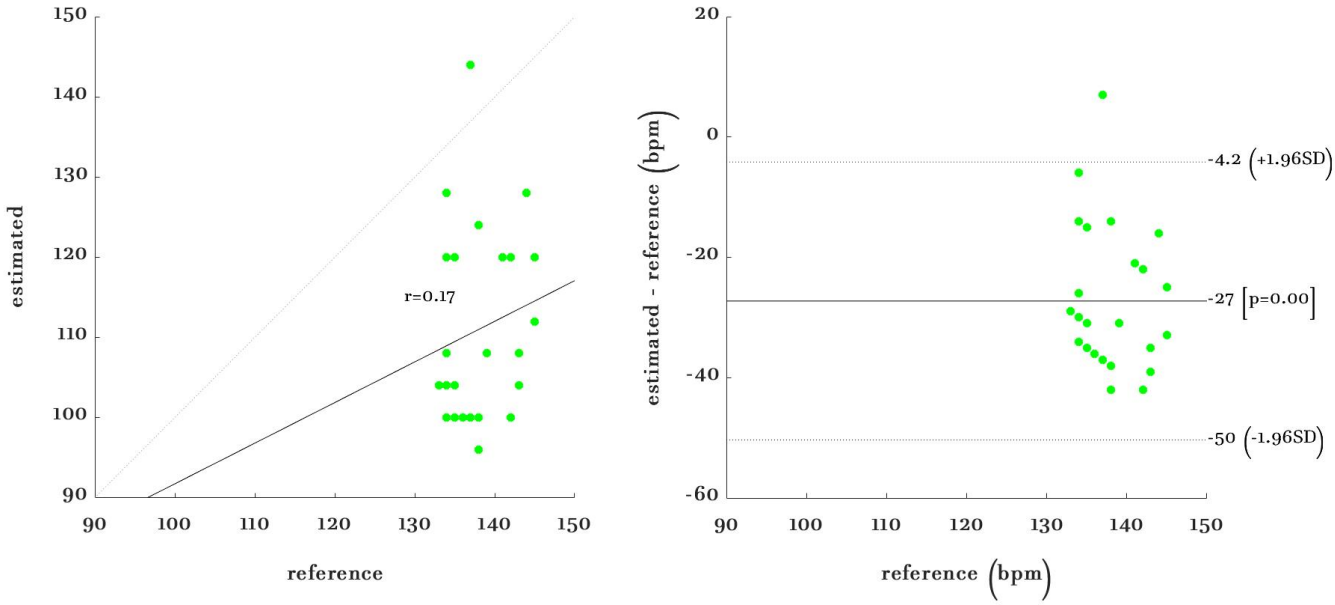

Figure 6.29: subject 5; Bland-Altman analysis plots

6.5.2 Light variations

In this second case, an example of what happens when ambient light varies over time: in fig 6.30 it's possible to observe ambient light variation on subject 5 face in 30 seconds.
Both extracted 6.31(a) and detrended traces 6.31(b) show variations in the amplitude of oscillations much greater than 7 pixels (validity threshold) in relatively short time windows (10 seconds).

Also in this case, the estimated results compared with the reference have been reported (fig. 6.32), in which it is observed that there is not only a difference in terms of absolute error but also the trend, more oscillating already at the level of ground-truth, it is not followed.

Fig. 6.33 shows the analysis of Bland-Altman, whereby most of the points are concentrated in the (mean ±SD) range, the mean value of the absolute error is around 11 bpm (absolute value).
Moreover, from the linear plot we observe an inverse proportionality of correspondence between estimated and reference data, confirmed by the negative sign of the Pearson coefficient, which in absolute value is 0.18, therefore shows that there is no correlation between the data.

The examples show how the movement and the variations of the light strongly influence the performance of the algorithm, which is therefore only reliable in short periods that are considered valid.

Figure 6.30: ROI plots every 5 seconds, subject 5

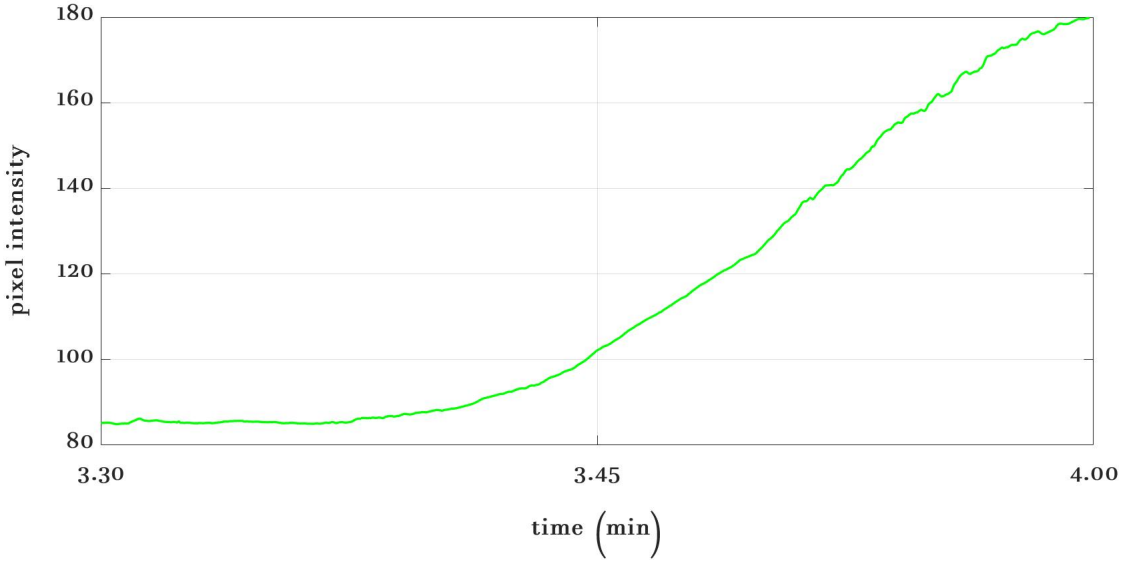

(a)

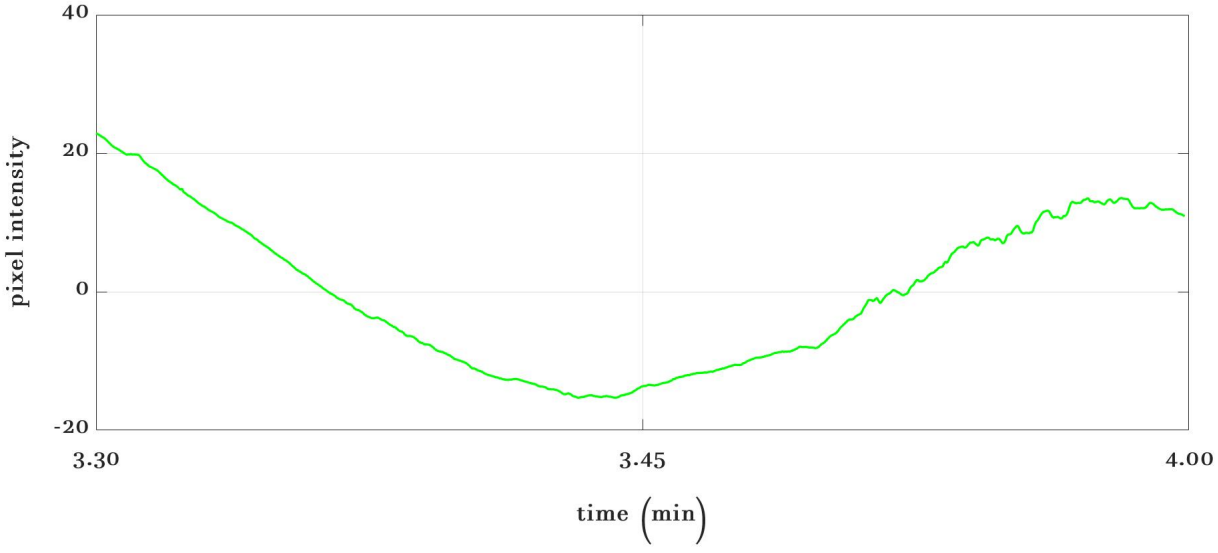

(b)

Figure 6.31: (a) averaged (b) detrended

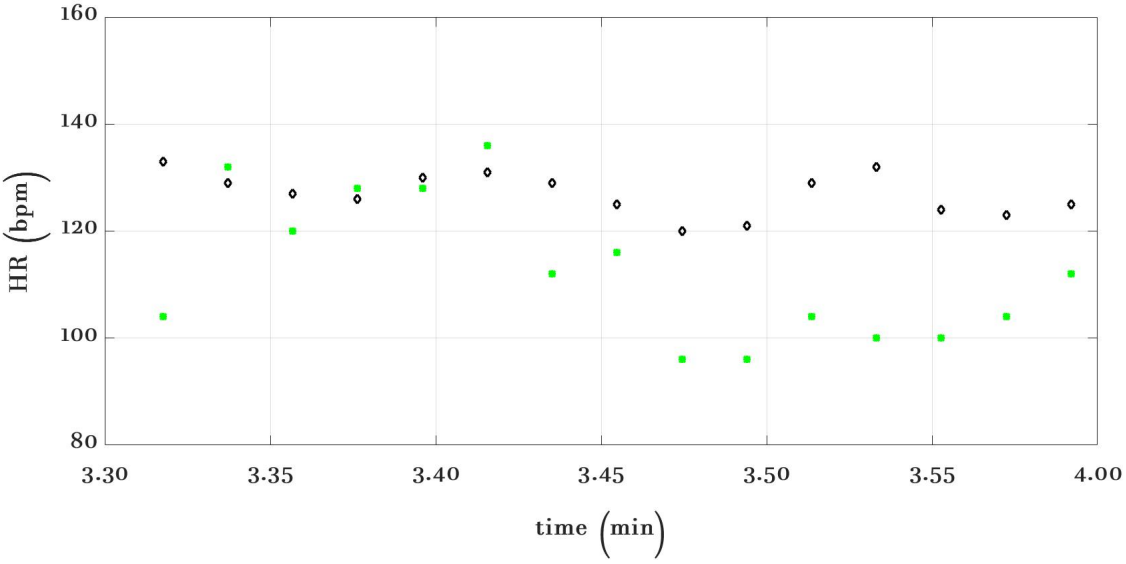

Figure 6.32: subject 5; HR results comparison

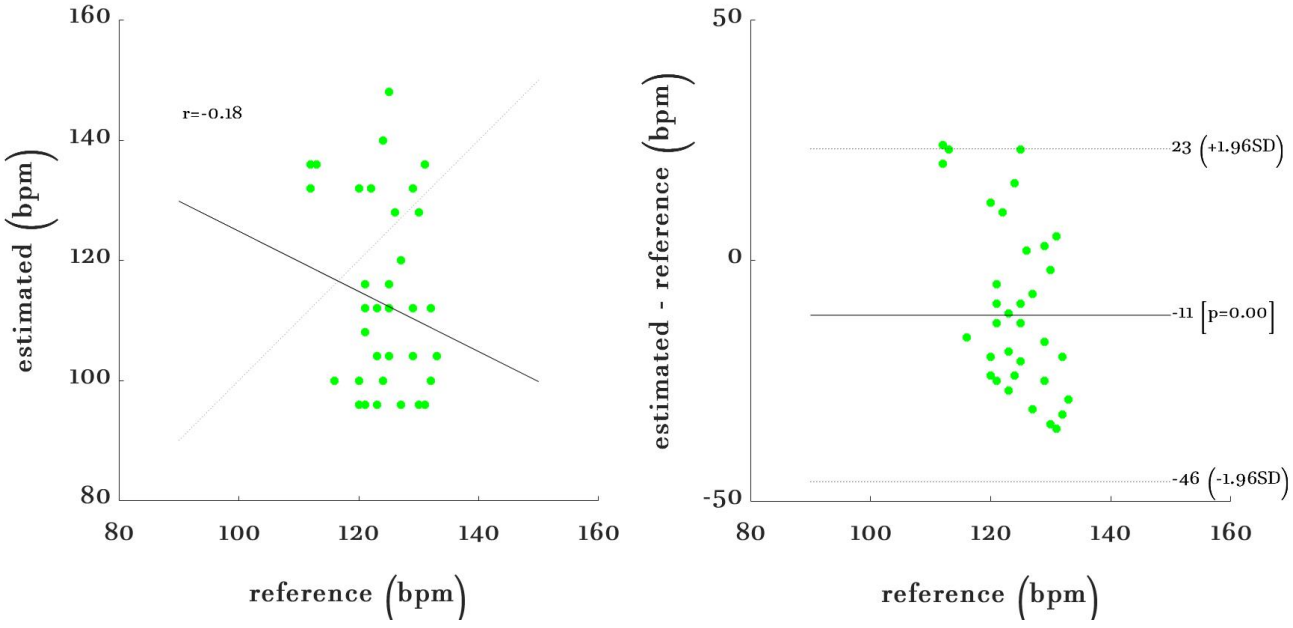

Figure 6.33: subject 5; Bland-Altman analysis plots

The state of the art presents some works in which the choice of validity periods is carried out automatically with more precise methods of an amplitude threshold of the oscillations, but a completely reliable contactless method has not yet been proposed and already used in the clinic for continuous monitoring; just think that the same gold standard, the pulse oximeter, guarantees an accuracy dependent on the presence or absence of movement.

Chapter 7

Conclusions and Future Works

The objective of an accurate estimate of the remote heart rate on healthy subjects born at term was achieved in a satisfactory and encouraging manner, under particular hypotheses.

As it emerges from the detailed description of the setup, from the multiple sessions of recordings necessary for the purpose and from the analysis of the results, the clinical context in which the work is inserted is as stimulating as it is complex.

Newborns are patients unable to express themselves and at the same time in need of communicating vital necessities, in one of the most delicate moments of their life: this means that there is a growing interest in exploiting the technological potentials in favor of support and optimization of medical intervention.

The greatest strength of the specific algorithm proposed is non-invasiveness, a very important aspect in order to continue the study adapting it to the case of intensive therapy in which the sensors used are more harmful than that of the pulse oximeter in terms of quantity and time of application (for example ECG sensors).

The limits of the instrument are different and partly linked to the nature of the scope of application: healthy infants are in fact continuously moving, as well as subject to episodes of crying and facial grimaces, the only channel of expression of distress and need.
The movement is indeed one of the most difficult aspects to manage in a system that assumes as hypothesis that the extraction of information from a specific region of interest framed and taken frontally with a fixed camera.
Fortunately, it is a partially solvable point implementing facial detection algorithms and therefore specific portions and tracking algorithms able to follow the region selected over time even when subjected to displacements.

The other factor that introduces variability in the accuracy of the method is the management of light, especially ambient light, that changes quickly and in an

uncontrollable way.
An example is represented by the video of the subject 5, for which it was impossible to identify periods of a minimum duration of 16 seconds in which the subject was relatively still and the light did not change too frequently.
This ”problem” can be tackled, especially with a view to implementing it in intensive care, managing the light in a more controlled manner and possibly using the artificial one with the necessary corrections to be taken into account during post-processing.

Regarding the future application in intensive care also, in which the amount of exposed skin is much greater than the changing table, it would be interesting to try to implement skin segmentation algorithms so as not to be bound to the front area alone and be able to exploit also periods in which other areas are visible, provided they are uniformly illuminated.

Another aspect to consider is that while at the changing table the babies are for relatively short periods of time during the screening and the puncture at the heel, in intensive care it is possible to acquire much longer and continuous recordings.

In addition to the improvements mentioned to optimize the proposed method and the benefits that can be drawn from the introduction in NICU, it is important to underline that contactless estimation of heart rate fits into the larger context of an objective assessment of pain.
It is therefore unquestionable to go ahead, in parallel, on the definition of a standardized method that, when it takes into account physiological parameters such as HR and oxygen saturation, foresees a quantification of the weight of this information compared to all the others related to behavioral parameters or facial expressions or crying analysis, highlighting any correlations or redundancies.

A natural development can also be the assessment of heart rate variability, used today in adults as a stress index in the assessment of health status, along with nutrition and physical activity. In infants this parameter is higher than in adults and may be indicative of the ability of the heart to adapt more or less quickly to external changes.

Summing up, the work presents itself as a small piece of a much wider project, which confidently looks to the use of innovation at the service of medicine, aimed in particular at patients in one of the most important phases of anatomical development of life.

Despite the encouraging results, there is still a lot of work to do and it is essential to continue in both technological and medical research.

Acknowledgments

My greatest feeling of gratitude goes to my parents, to love and support me in every possible way, especially during the last months of this academic journey.
Thanks to the great, little, Nihal for the inexpressible emotional force.

Thanks to Emilia Parodi, pediatrician in Mauriziano Hospital and Marco Gavelli, engineer at Istituto Superiore Mario Boella (ISMB) for the idea that led to the birth of this great and important project in which technology meets medicine.

Thanks to Jessica Munarin, collaborator and friend, for technical and moral support, patience and commitment during the recording sessions.

Thanks to Enrico Baccaglini and Riccardo Scopigno for the opportunity and trust; to all ISMB colleagues for the serene and collaborative work environment.

Thanks also to Dr. Frigerio, head of neonatology and to all the hospital staff for trust and availability.

Thanks to Professor Molinari for the knowledge acquired in his signal processing and medical images lectures and for the opportunity.

A very huge thanks to Mauricio Villarroel and Joao Jorge, Department of Biomedical at Oxford University for the constant advice, comparisons and the enormous interest shown.

Turning to those who contributed less directly but not for this less important, a special thanks to Nicole, irreplaceable friend, for the enormous emotional strength and at the same time deep sensitivity.

Thanks to my family, friends and classmates, who in these months have had patience and understanding, active interest and inexhaustible stimuli to overcome difficulties with a smile.

The last thanks goes to myself, for trying to get the best out of every situation by growing in skills and knowledge, without ever forgetting the human side: the most stimulating element of biomedical engineering.

Bibliography

[1] Wiley Blackwell. *Advanced Paediatric Life Support: The Practical Approach. 4th ed.* 2004.

[2] A.K.Dum et al. Dynamic imaging of cerebral blood flow using laser speckle. *J.Cereb. Blood Flow Metab.*, 21(3):195–201, 2001.

[3] Alessandro R. Guazzi et al. Non-contact measurement of oxygen saturation with an RGB camera. *OSA - BIOMEDICAL OPTICS EXPRESS*, 6(9), 2015. doi: 10.1364/BOE.6.003320.

[4] Aymen A.AlianM.D. et al. Photoplethysmography. *ELSEVIER - Best Practice Research Clinical Anaesthesiology*, 28(4):395–406, December 2014. doi: https://doi.org/10.1016/j.bpa.2014.08.006.

[5] J. Allen et al. Photoplethysmography and its application in clinical physiological measurement. *IOP Publishing - Physiological Measurement*, 28, 2007. doi: DOI:10.1088/0967-3334/28/3/R01.

[6] J. O'Doherty et al. Sub-epidermal imaging using polarized light spectroscopy for assessment of microcirculation. *Skin Res. Technology*, 13(4):472–484, 2007.

[7] K.Wardell et al. Laser Doppler perfusion imaging by dynamic light scattering. *IEEE Trans. Biomed. Eng.*, 40(4):309–316, April 1993.

[8] L. Scalise et al. Heart rate measurement in neonatal patients using a webcamera. *Medical Measurements and Applications Proceedings (MeMeA), 2012 IEEE International Symposium on*, 2012. doi: 10.1109/MeMeA.2012.6226654.

[9] L.Kong et al. Non-contact detection of oxygen saturation based on visible light imaging device using ambient light. *OSA - OPTICS EXPRESS*, 21(15), 2013. doi: 10.1364/OE.21.017464.

[10] Lonneke A.M. Aarts et al. Non-contact heart rate monitoring utilizing camera photoplethysmography in the neonatal intensive care unit — A pilot study. *Elsevier; Early Human Development*, 89:943–948, 2013.

[11] L.V. Wang et al. Multiscale photoacoustic microscopy and computed tomography. *Nat. Photonics*, 3(9):503–509, 2009.

[12] Melis et al. Automated newborn pain assessment framework using computer vision techniques. *ICBRA 2017*.

[13] Poh et al. Non-contact, automated cardiac pulse measurements using video imaging and blind source separation. *OPTICS EXPRESS*, 2010.

[14] Poh et al. Advancement in Noncontact, Multiparameter Physiological Measurements Using a Webcam. *IEEE TRANSACTION ON BIOMEDICAL ENGINEERING*, 58(1), January 2011.

[15] Tarassenko et al. Non-contact video-based vital sign monitoring using ambient light and auto-regressive models. *IOPscience*, 2014. doi: http://iopscience.iop.org/0967-3334/35/5807.

[16] Verkruysse et al. Remote plethysmographic imaging using ambient light. *Opt. Express*, 16:21434–21445, 2008.

[17] Wieringa et al. Contactless Multiple Wavelength Photoplethysmographic Imaging: A First Step Toward "SpO2 Camera" Technology. *Ann. Biomed. Eng.*, 33:1034–1041, 2005.

[18] Yu Sun et al. Photoplethysmography Revisited: From Contact to Noncontact, From Point to Imaging. *IEEE TRANSACTION ON BIOMEDICAL ENGINEERING*, 63(3), March 2016.

[19] Alrick B. Hertzman. The blood supply of various skin areas as estimated by the photoelectric plethysmograph. 1938.

[20] Kenneth Humphreys and Tomas Ward. Noncontact simultaneous dual wavelength photoplethysmography: A further step toward noncontact pulse oximetry. *AIP Review of Scientific Instruments*, 78, 2007. doi: https://doi.org/10.1063/1.2724789.

[21] M. Villarroel et al. J. Jorge. Non-contact monitoring of respiration in the neonatal intensive care unit. *IEEE 12th International Conference on Automatic Face Gesture Recognition*, 2017. doi: 10.1109/FG.2017.44.

[22] Douglas G Altman J Martin Bland. Measuring agreement in method comparison studies. *SAGE journals*, 8(2), 1999.

[23] Marlies van den Born et al. John H.G.M. Klaessens. Development of a baby friendly non-contact method for measuring vital signs: First results of clinical measurements in an open incubator at a neonatal intensive care unit. *Proc. of SPIE (Digital Library)*, 8935, 2017. doi: 10.1117/12.2038353.

[24] Garetti *et al.* Lago. Procedural pain in neonates: the state of the art in the implementation of national guidelines in Italy.. *Pediatric Anesthesia*, 23(5): 407–414, 2013.

[25] Lalit K. Mestha. Towards Continuous Monitoring of Pulse Rate in Neonatal Intensive Care Unit with a Webcam. *Engineering in Medicine and Biology Society (EMBC), 2014 36th Annual International Conference of the IEEE*, 2014. doi: 10.1109/EMBC.2014.69444554.

[26] Kattwinkel J Atkins DL Chameides L Goldsmith JP *et al.* Perlman JM, Wyllie J. Part 11: Neonatal resuscitation: 2010 International Consensus on Cardiopulmonary Resuscitation and Emergency Cardiovascular Care Science With Treatment Recommendations.. 2010.

[27] Cindy Stanfield. *Fisiologia*. EdiSES, 2012.

[28] J. A. Lemons *et al.* Prevention and management of pain and stress in the neonate. *Pediatrics*, 105(2), 2000.

[29] Ola Didrik Saugstad *et al.* Response to resuscitation of the newborn: Early prognostic variables. *ACTA PAEDIATRICA*, 94(7), 2005.

[30] Giovanni Zaninetta and SICP Presidente. La legge 38/2010 e le cure palliative italiane. *La voce della SIC*, 2010.